Published in final edited form as:
Adv Drug Deliv Rev. 2014 February ; 0: 58–73. doi:10.1016/j.addr.2013.09.008.

Stimuli-responsive cross-linked micelles for on-demand drug delivery against cancers

Yuanpei Li[1,‡,*], **Kai Xiao**[1,‡], **Wei Zhu**[2], **Wenbin Deng**[1], and **Kit S. Lam**[1,**]

[1]Department of Biochemistry & Molecular Medicine, UC Davis Cancer Center, University of California Davis, Sacramento, CA 95817, USA

[2]Department of Cardiology, the First Affiliated Hospital of Zhejiang University, School of Medicine, Zhejiang University, Hangzhou, 310003, China

Abstract

Stimuli-responsive cross-linked micelles (SCMs) represent an ideal nanocarrier system for drug delivery against cancers. SCMs exhibit superior structural stability compared to their non-crosslinked counterpart. Therefore, these nanocarriers are able to minimize the premature drug release during blood circulation. The introduction of environmentally sensitive crosslinkers or assembly units makes SCMs responsive to single or multiple stimuli present in tumor local microenvironment or exogenously applied stimuli. In these instances, the payload drug is released almost exclusively in cancerous tissue or cancer cells upon accumulation via enhanced permeability and retention effect or receptor mediated endocytosis. In this review, we highlight recent advances in the development of SCMs for cancer therapy. We also introduce the latest biophysical techniques, such as electron paramagnetic resonance (EPR) spectroscopy and fluorescence resonance energy transfer (FRET), for the characterization of the interactions between SCMs and blood proteins.

Keywords

Micellar nanoparticles; Drug delivery; Stimuli-response; Crosslink; FRET; EPR spectroscopy

Introduction

Nanotechnology offers new opportunities for diagnosis and treatment of a variety of cancers [1–5]. Multifunctional nanoparticles possessing functions including tumor targeting [6–10], imaging [11–14] and therapy[10, 15–17] are under intensive investigation aiming to overcome limitations associated with conventional cancer diagnosis and therapy [18–20]. Over the past decade, polymeric micelles have been extensively investigated as nanocarriers to deliver conventional anticancer drugs. These nanoparticles provide several distinct advantages for the drugs, such as improved solubility, prolonged *in vivo* circulation time and preferential accumulation at tumor site via the enhanced permeability and retention effect

[*]Corresponding author. liyuanpei@gmail.com (Y. Li), Tel.: +1 916 734 0905; fax: +1 916 734 6415. [**]Corresponding author. kit.lam@ucdmc.ucdavis.edu (K. S. Lam), Tel.: +1 916 734 0910; fax: +1 916 734 7946.
[‡]Yuanpei and Kai contributed equally to this work

[21–24]. Despite the recent progress in the research of micellar nanoparticles, some shortcomings are gradually revealed which may limit their application in clinic. In blood circulation, blood proteins and lipoproteins such as high density lipoprotein (HDL), low density lipoprotein (LDL), very low density lipoprotein (VLDL) and chylomicron may interact with the polymeric micellar nanoparticles [25]. This process can result in the early disintegration or aggregation of micelles and premature drug release [26]. Besides, polymeric micelles are thermo-dynamic self-assemble system which has a well-known equilibrium existed between micelles and unimers (assembly unit) in aqueous condition. After being injected into the blood stream, conventional self-assembled polymeric micelles are susceptible to dilution below the critical micelle concentration (CMC). This may lead to the dissociation of micelles into unimers.

Cross-linking strategy has been utilized to solve the above mentioned stability problems following the pioneer work by Wooley's group [27]. Since then, this strategy has been exploited by a number of other groups [28–33]. Covalent cross-links between specific domains of the micelles are formed in order to improve the micelles' structural stability suitable to drug delivery rather than the weak non-covalent intermolecular hydrophobic interactions existing in the conventional polymeric micelles that facilitate polymer micelles assembly and integrity [27]. To be more effective, anticancer drugs should be released exclusively in tumor tissue or inside tumor cell. However, excessively stabilized micelles may prevent the drug from releasing to target sites, thus reducing the therapeutic efficacy [28, 29]. Stimuli-responsive cross-linked micelles (SCMs) are introduced to improve the drug delivery [30–33]. SCMs exhibit unique stability in blood circulation and can better retain the drug contents. The utilization of environmentally sensitive crosslinkers or assembling units makes SCMs responsive to single or multiple stimuli in the microenviroment of tumor site or inside the tumor cells [34, 35] or the application of exogenous stimuli (Fig. 1). The cleavage of the intra-micellar crosslinkage or disassembly of the micelles responding to stimuli leads to exclusively drug release in the target site [36, 37]. The special micelles are often called 'smart' or 'intelligent' micellar nanoparticles. This review briefly summarizes the recent advances in stimuli-responsive crosslinked micellar nanocarriers with the main focus on the design, characterization, crosslink strategy, protein interaction, stimuli-sensitive release mechanism and preclinical evaluation.

Main text

1. Design of stable SCMs with single or multiple responsive properties

The basic elements need to be considered in the design of SCMs include how and where to introduce crosslinkages to the micelles and how to endow the micelles with responsiveness to the microenvironments of the target sites or exogenous stimuli. The crosslinkage can be introduced at the hydrophilic shell [38, 39], hydrophobic core [26, 40, 41] or core-shell interface [35, 42] of the micelle via chemical crosslink, photo crosslink or polymerization after the micelle formation via self-assembly in aqueous solution. Recently, *in situ* cross-linking approach has been reported by several groups. In this case, one or two types of crosslinkable pendants are introduced to the assembly units so that the micelles can be crosslinked spontaneously during the micelle formation [43, 44]. The reported stimuli for drug delivery include pH, temperature, enzymes, electrolytes, redox (reduction/oxidization), ultrasound, light and magnetic field [45–47]. Very recently, a few studies have been succeeding in systemically applying exogenous stimuli via FDA approved agents, such as N-Acetylcysteine (a reducing agent) and mannitol (a cis-diol) [43, 44]. The responsiveness of SCMs refers to their ability to receive, transmit one or multiple types of above mentioned stimuli, and respond with desirable effects, including degradation, swelling/collapsing, dissolution/precipitation and eventually triggering the drug release from the nanocarriers. In order to make the crosslinked micelles responsive to tumor local environments, polymers

with intrinsic responsive properties to pH, temperature, or redox conditions have been used to design SCMs. Furthermore, various cleavable crosslinkages (e.g. disulfide bonds [44], pH cleavable [48] or hydrolysable ester bonds [26]), have also been utilized to synthesize crosslinked micelles. An overview of the SCMs including the assembly units, preparation methods, crosslinking strategy, stimuli response and their applications are given in Table 1.

1.1 Hydrolysable SCMs—Several biodegradable polymers, such polylactate (PLA), polycaprolactone (PCL) have been exploited to design hydrolysable crosslinked micelles for anticancer drug delivery. Talelli *et al* reported such micelles via the self-assemble of poly(ethylene glycol)-b-poly[N-(2-hydroxypropyl) methacrylamide-lactate] (mPEG-b-p(HPMAm-Lacn)) diblock copolymers in aqueous solution when heated above the critical micelle temperature (CMT) [46, 49]. 30~40% w/w of doxorubicin was loaded into the micelles though the conjugation of a DOX methacrylamide derivative (DOX-MA) to the micelles core followed by core crosslink via free radical polymerization. DOX-MA is hydrolysable under acidic conditions (mimicking the microenvironment within the tumor and in the intracellular organelles leading to micelle disintegration). An enhanced tumor accumulation and a prolonged circulation time were obtained after intravenous administration of these micelles because of their relatively small particle size (60–80 nm) and the intra-micellar crosslinkages. In the drug release studies, it was observed that the crosslinked micelles released the entire drug payload after 24h incubation at pH 5 and 37 °C, while around 5% of doxorubicin was released during the same period of time when incubated at pH 7.4 and 37 °C. Furthermore, the crosslinked micelles with covalently bound DOX showed higher cytotoxicity against B16F10 and OVCAR-3 cells and better therapeutic efficacy in B16F10 melanoma carcinoma mice models than both free DOX and DOX-MA. Lee et al demonstrated a biocompatible and pH-hydrolyzable shell cross-linked polymer micelle for DOX delivery [50]. The micelles were self-assembled by triblock copolymer of poly(ethylene glycol)-poly(L-aspartic acid)-poly(L-phenylalanine) (PEG-PAsp-PPhe) forming core-shell-corona model with the PEG outer corona, the PAsp middle shell, and the PPhe inner core. Bifunctional ketal cross-linkers with the primary amines reacted with O-acylurea in Asp moieties forming crosslinkages at the shell of the micelles. Transmission electron microscopy (TEM) and dynamic light scattering (DLS) results implied that the PEG outer corona confines the shell cross-linking reaction within the PAsp middle shells, preventing the formation of intermicellar aggregates. The shell cross-links act as a diffusion barrier for low molecular weight compounds and may be effective in reducing the premature drug release at pH 7.4. It was found that the shell crosslinked micelles showed high physical stability even after the addition of strong detergent in fluorescence spectroscopy experiments. Meanwhile, the hydrolysis kinetics study demonstrated that the half-life of ketal cross-linked micelles at pH 5.0 was 74-fold faster than that at pH 7.4. As a result, the DOX release from the micelles was faster at pH 5.0 than that at pH 7.4.

1.2 Redox sensitive SCMs—Given the unique characteristics of redox state in the body, reducible linkages have been widely applied to smart micellar nanoparticles system. The concentration of a thiol-containing tripeptide called glutathione (GSH) in cytoplasm could be 100–1000 fold higher than that in the extracellular environments and blood pool [35, 51, 52]. Meanwhile, in some particular tumor cells, the concentration of GSH is about seven times higher than that in the normal cells [52, 53]. The high concentration of GSH in cytoplasm could lead to the cleavage of disulfide bond to free thiols via the redox reaction, which is the mechanism of intracellular drug release for redox sensitive cross-linked micelles. So far, researchers have used the disulfide bond cross-linked smart micelles to deliver doxorubicin (DOX) [54], paclitaxel (PTX) [44], methotrexate (MTX) [35], vincristine (VCR) [55], DNA [56] and siRNA to the target site following the pioneer effort of Kataoka group. Lipoic acids have been utilized as crosslinkable groups to design

reduction sensitive cross-linked nanoparticles [29]. For instance, Zhong et al reported a type of disulfide crosslinked nanoparticle assembled *via* dextran-lipoic acid conjugates followed by catalyzing the crosslinking reaction via 10 mol% dithiotheitol (DTT) relative to the lipoyl units in phosphate buffer (pH 7.4, 10 mm) [29]. It was found that monodispersed nanoparticles with average sizes ranged from 85.3 to 142.5 nm before cross-linking and shrunk by 20–35 nm after cross-linking. Notably, the crosslinked dextran nanoparticles (C-DNPs) exhibited superior drug loading efficiency in contrast with the non-crosslinked dextran nanoparticles. In the *in vitro* drug release studies, they found that the release of DOX from C-DNPs decreased to minimal about 10% even after extensive dilution, but over 90% of the DOX was released in 11 h after the addition of 10 mM DTT, which mimicks the intracellular reductive environment. Our group has recently developed a novel type of reduction-sensitive disulfide crosslinked micelles, which exhibit excellent stability, prolonged blood circulation time, and minimal drug premature release properties [44]. We introduced four cysteines to polylysine backbone of our previously reported linear dendritic polymer (called telodendrimer) PEG^{5k}-CA_8, resulting in a well-defined amphiphilic thiolated telodendrimer. The thiolated telodendrimers were then self-assembled to form micelles with particle size of around 20 nm followed by air oxidation of free thiols to intra-micellar disulfide crosslinkages (Fig. 2). Dynamic light scattering was applied to study the stability of the micelles via monitoring the change of micellar particle size. In the presence of sodium dodecyl sulfate (SDS), an ionic-detergent which is known to disintegrate polymeric micelles [35], the disulfide cross-linked micelles retained their particle size for days while the corresponding non-cross-linked micelles dissociated rapidly as evidenced by the immediate disappearance of the measured particle size signal (Fig. 3A). However, after the addition of SDS and GSH, the particle size of the cross-linked micelles was stable in the first 30 min but suddenly disintegrated within 10 sec, indicating that the reduction of a critical number of disulfide bond leads to a rapid dissociation of the micelle. The level of crosslink and therefore *in vivo* stability of such micelles can be fine-tuned conveniently by varying the ratio between thiolated and non-thiolated telodendrimers. These characteristics of the cross-linked micelles may endow the drug nanocarriers prolonged circulation time and triggered drug release at the tumor site and inside the cancer cells with high reductive potential. We found that the release of encapsulated paclitaxel from disulfide cross-linked micelles was slower than that from non-crosslinked micelles in PBS solution. The drug release rate of the non-crosslinked micelles remained unchanged after adding GSH (10 mM) at a specific release time (5h), whereas that of the cross-linked micelles showed an dramatic increase after the addition of GSH to cleave the disulfide bond (Fig. 3B). In addition, N-acetylcysteine (NAC), an FDA approved reducing agent has been demonstrated to possess similar effect as GSH in breaking down the disulfide bond. So it has the potential to act as a triggering agent for the drug release from disulfide crosslinked micelles after these micelles have accumulated in the tumor site (Fig. 4). So far, several polymeric micelle systems with ionic core containing biodegradable crosslinkages such as disulfide bond have been designed, synthesized and applied for the delivery of gene [57, 58] or chemotherapeutic agents [59]. A new class of polymeric micelle, called the polyion complex (PIC) micelle, has been developed by Kataoka et al. They have selectively added thiol groups to the lysine repeat units resulting in poly(ethylene glycol)-block-poly-(L-lysine) (PEG-P(Lys)) [57]. During the self-assemble of PEG-P(Lys) to a PIC micelle, the free thiols remained in the lysine core were oxidized to form disulfide bond. The disulfide bond can be reversibly cleaved by reducing agents such as GSH or DTT. Another kind of micelles with ionic core containing disulfide bond has been reported by Kim et al based on block ionomer complexes (BIC) of poly(ethylene oxide)-*b*-poly(methacylic acid) (PEO-*b*-PMA) and divalent metal cations (Ca^{2+}) as templates [59]. They used cystamine as a biodegradable cross-linker to form the disulfide bond in the ionic core. These micelles (with particle size of 100–220 nm

in diameter) exhibited a superior doxorubicin loading (50% w/w) in the ionic core and significantly increased cytotoxicity against human A2780 ovarian carcinoma cell.

1.3 pH sensitive SCMs—In recent years, pH-sensitive micelles have emerged as an important class nanocarrier for drug delivery based on the subtle pH changes in the human body. For example, the pH in the stomach is pH 1–2 compared with that in intestine (pH 5–8). The pH of the extracellular in the tumor site is slightly acidic (pH 6.5–7.2) while the pH value in blood and normal tissue is about 7.4. The endosome has a pH ranges from 5.0 to 6.5 and the pH in lysosome is even lower varying from 4.5 to 5.0. The pH-sensitive SCMs can target tumor site or the organelles in the tumor cells and release loaded drug due to the pH difference existing in the body [60–63]. Chan and co-workers have reported a type of acid-labile core cross-linked micelles for pH-triggered drug release composed of poly(hydroxyethyl acrylate)-block-poly(n-butyl acrylate) (PHEA-b-PBA) [40]. The core of the micelles was cross-linked via the reversible addition-fragmentation chain transfer (RAFT) polymerization of a divinyl functionalized degradable monomer from the living polymer chains which can be triggered to disintegrate by a pH-dependent manner. There was no big change in the particle size and morphology of the cross-linked micelles compared with the original non-crosslinked micelles determined by TEM and DLS. During the cross-linking process, high drug loading capacity (up to 60 wt % of the copolymer weight) was achieved because of the π-π interactions between doxorubicin and the crosslinker's phenyl ring. Both cleavage and drug release rates at acidic pH were significantly higher than those at neutral pH. The pH-sensitive micelles capable of releasing drugs at slightly acidic pHs such as those found in extracellular fluids or intracellular endosomes of tumors are promising for anti-tumor chemotherapy. Du and colleagues reported a type of shape-persistent polymeric vesicle with pH-tunable membrane permeability. The vesicles were formed by the self-assembly of a pH-responsive, hydrolytically self-cross-linkable copolymer, poly(ethylene glycol)-b-poly((2-(diethylamino) ethyl methacrylate)-s-(3-(trimethoxysilyl) propyl methacrylate)) (PEG-b-P(DEA-s-TMSPMA)) [64]. Siloxane was utilized to crosslink the polymeric vesicle based on the further reaction of -$Si(OD)_3$ groups. The mean diameter (D_h) of the vesicles is 630±250 nm at neutral pH while the D_h increased monotonically under pH value below 7. Furthermore, the walls of the vesicles swell along with the protonation of the DEA residues.

1.4 Multi-responsive SCMs—Recently, novel SCMs with multi responsiveness properties have been designed to deliver drugs to the complicate *in vivo* microenvironments. The SCMs' ability to respond to multiple stimuli, for instance, pH/reduction, temperature/reduction, temperature/pH and pH/cis-diol are introduced in the following section.

1.4.1 pH/reduction sensitive SCMs: A novel class of SCMs that are responsive to acidic and reductive stimuli was synthesized by Chen and co-workers [65]. The micelles with particle size of 60–100 nm were self-assembled via the polymers of PEG and 2,2'-dithio-diethanol diacrylate, 4,4'-trimethylene dipiperidine. The disulfide bonds and tertiary amines on the backbone of poly(β-amino ester) make SCMs have the characteristic of pH and reduction dual-sensitivity. The drug release profile of the DOX-loaded SCMs was monitored by UV-vis spectrometry at 480 nm at different time. About 30% of the entrapped DOX was released within 48 h in PBS solution at pH 7.4, while at pH 6.5, a 50% release in the first 6 h and up to 75% release in 48 h was observed. These results indicated that the tertiary amines in the core prevented the loaded DOX from diffusing to the outside of the smart micelles at physiological pH which maintained the core-shell structure of the micelles. The difference response to pH ranging from 7.4 to 6.5 corresponding to the change from extracellular pH to early endosomal pH suggested those SCMs are a suitable intracellular drug delivery system. As described before, the reducing agents can trigger cleavage of the disulfide bonds and lead

to a burst release of loaded-drug. DTT, a reducing agent, was used in the reduction-sensitive study of the smart micelles. The DOX released at a low rate similar to that in PBS at pH 7.4 in 0.1mM DTT solution compared to more than 40% DOX release in 1mM DTT. When the concentration of DTT reached 5 mM, about 60% DOX was released within first the 6 h and up to 80% DOX release was measured with 48 h. Shuai et al also demonstrated a highly packed interlayer-crosslinked micelle (HP-ICM) with pH and reduction dual sensitivity prepared from a triblock copolymer of monomethoxy polyethylene glycol (mPEG), 2-mercaptoethylamine (MEA)-grafted poly(laspartic acid) (PAsp(MEA)), and 2-(diisopropylamino)ethylamine (DIP)-grafted poly(l-aspartic acid) (PAsp(DIP)) [62]. Poly(BLA) aminolysis with MEA and DIP were utilized to introduce, disulfide bonds and imine bonds responding to acidic pH (pH 5.5) and a reducing agent tris(2-carboxyethyl)phosphine (TCEP), respectively. The HP-ICM was highly stable and drug release rate was extremely low at pH 7.4. However, in the presence of reducing agent and an acidic pH (~5), the HP-ICM was dissociated and the loaded drug was released significantly faster.

1.4.2 Temperature /pH sensitive SCMs: A novel type of temperature and pH sensitive crosslinked micelles was developed by Babin and coworkers using an amphiphilic diblock copolymer of $PDMAEMA_{54}$-b-P(MMA_{55}-co-MMA_{19}) [66]. The shell cross-linked reverse micelles (SRCM) were obtained via photo-cross-linking upon UV irradiation at $\lambda > 310$ nm. The halide groups of SRCM initiated the grafting of styrene and dimethylaminoethyl methacrylate (DMAEMA) on the surface of the nanoparticles *via* atom transfer radical polymerization (ATRP). The resulting nanoparticles were sensitive to the changes in pH and temperature as well as UV irradiation. Zhang et al have reported the synthesis of dual pH- and temperature-sensitive SCMs via the self-assemble of thermoresponsive block copolymer ($PAGA_{180}$-b-$PNIPAAM_{350}$) [67]. 3,9-divinyl-2,4,8,10-tetraoxaspiro[5.5]-undecane was used as an acid-labile crosslinking agent to generate the dual sensitive crosslinked nanoparticles. The resulting micelles were very stable at pH ranging from 6 and 8.2 but could be degraded at acidic conditions.

1.4.3 Temperature/reductive sensitive SCMs: A core cross-linked micelle system possessing sensitivity to temperature and reduction was reported by Jiang et al. These micelles were synthesized in a one-pot manner via RAFT copolymerization of *N*-isopropylacrylamide (NIPAM) and bis(2-methacryloyloxyethyl) disulfide (DSDMA) difunctional monomers using PAEMA as the macromolecular RAFT agent [41]. The obtained micelles were biocompatible and bioactive, since the amino groups in outer coronas of the micelles were further conjugated with carbohydrate and biotin as the targeting moieties. The temperature and reduction sensitivity of the micelles were demonstrated via the rupture of disulfide bonds in the presence of DTT and the shrinking of micelle cores when heating above the phase transition temperature of PNIPAM. These results indicated that the temperature and reductive sensitive SCMs have the potential to be used for targeted and controlled drug delivery.

1.4.4 pH/cis-diol sensitive SCMs: Boronate esters formed by boronic acids and diols possess dual sensitivity to pH value and competing diols [68–71]. Catechols are considered as an excellent reactant in the forming process of boronate esters. We have developed a novel type pH/cis-diol sensitive SCMs based on this principle for anticancer drug delivery [43]. A series of boronate cross-linked micelles with particle size of 20–30 nm were synthesized using equal molar ratios of the boronic acid- and catechol- containing telodendrimers (Fig. 5). Among them, BCM4 formed by the telodendrimer pair of PEG^{5k}-NBA_4-CA_8 and PEG^{5k}-$Catechol_4$-CA_8 showed superior stability with no significant particle size changes in the presence of either 50% (v/v) human plasma in 24 h or 2.5 mg/mL SDS

solution. However, a rapid decrease of particle size occurred in SDS when the external pH value decreased to 5.0 or mannitol (100 mM, a safe FDA approved drug for diuresis) was added into the solution, indicating that the cleavage of critical percentage of boronate (Fig. 6A). PTX was used as model drug to compare the release kinetics of the reversible boronate cross-linked micelles and the non-crosslinked micelles (NCM). As the boronate formed by boronic acids and catechols could be disassembled in acidic environment or in the presence of mannitol, it was suggested that the drug release from these micelles could be triggered inside endosomes of tumor cells with an acidic pH or at the tumor sites with exogenously administered mannitol. Within the first 5 h, the PTX release of BCM4 was much slower than that of NCM as shown in Fig. 6B. However, the BCM4 showed a burst PTX release upon the addition of 100 mM mannitol or the pH of the medium was adjusted to 5.0 at the 5 h time point. Furthermore, the combination of acidic pH and 100 mM mannitol could greatly accelerate the PTX release of the BCM4 micelles. This novel dual pH/cis-diol responsive nanocarriers to exhibited great promise for drug delivery accompanying with minimal premature drug release at physiological glucose level (2–10 mM) and physiological pH values (pH 7.4) in blood circulation but can be activated to release drug on demand at the acidic tumor microenvironment or in the acidic cellular compartments upon uptake into target tumor cells.

The SCM-based nanocarriers take advantage of the unique endogenous and exogenous stimuli and incorporate them into micelle-based drug delivery systems to precisely regulate the drug release. Although promising, addition of stimuli-responsive crosslinkers to the nanocarrier will add complexity and cost to their preparation. Therefore, robust processes that facilitate scale-up synthesis and manufacturing will undoubtedly accelerate the translation of SCMs into the clinics.

2. Characterizations of the interaction between SCMs and blood proteins

Blood proteins or lipoprotein particles may interact strongly with micellar nanoparticles, resulting in the dissociation of the nanoparticles and premature drug release. To get a better understanding of the interaction between SCMs and blood proteins, site-specific labeling with spin probes and fluorophores combined with electron paramagnetic resonance (EPR) spectroscopy and fluorescence resonance energy transfer (FRET) measurements were applied to monitor the assembly structure and dynamics within nanoparticles. EPR is a sensitive spectroscopic technique for studying materials with unpaired electrons. FRET, often call “molecular ruler”, is a distance dependent physical process by which an excited donor chomophore may transfer energy to an acceptor chomophore through nonradiative dipole-dipole coupling. Both EPR and FRET provide unique capabilities to probe the order within nanoparticles in a highly sensitive manner [25].

We combined site-specific nitroxide spin labeling and fluorescence labeling techniques with EPR spectroscopy and FRET technique, respectively, to probe the multiple dynamic processes occurring within nanoparticles during interaction with blood proteins. These techniques enable us to quantitatively analyze the dynamic changes in assembly structure, local stability and cargo diffusion of a class of novel telodendrimer-based micellar nanoparticles in human plasma and individual plasma components [25]. The site-specific spin label reporter system was developed via attaching 2,2,6,6-tetramethylpiperidinyloxy (TEMPO) to two specific sites on the PEG^{5k}-CA_8 telodendrimers (Fig. 7) which can self-assemble in aqueous solution forming a typical core-shell spin-labeled non-cross-linked micellar nanoparticles, named S-NCMN1 and S-NCMN2. S-NCMN1 had the spin labels on its surface while the spin labels located closely at the core-shell interface were called S-NCMN2. Using the same method, TEMPO was introduced to the lysine proximal to the oligocholic acids of PEG^{5k}-Cys_4-CA_8 resulting in spin-labeled disulfide cross-linked nanoparticles (S-DCMN2) (Fig. 7). S-NCMN2 showed a sharp spectrum as the micelles

immediately lost its assembly order indicating a signal of increased intensity after incubation in human plasma. However, the EPR signal of S-NCMN1 and S-DCMN2 increased slightly over time. LDL, HDL, VLDL, chylomicron and human serum albumin were chosen as the blood components to investigate their interactions with the micelles. The results indicated that lipoprotein particles e.g. LDL, VLDL and chylomicron could interact with noncrosslinked micelles strongly and eventually broke down the micelles (Fig. 8). We also revealed that we could minimize the interactions of micellar nanoparticles with blood proteins though introducing disulfide crosslinkages into the nanoparticles and activate these interactions by using reducing agents to cleave the disulfide bonds subsequently.

We constructed thee position-specific FRET-based fluorescence reporter systems to monitor the dynamic changes in local proximity within nanoparticles upon interaction with blood proteins (Fig. 9). The first FRET system was developed by a green carbocyanine dye DiO (donor) physically encapsulated in the core of the disulfide cross-linked smart micelles without spin labeled and a red-orange dye rhodamine B (acceptor) covalently conjugated to the telodendrimer units. The second FRET system consisted of DiO (donor) and a red-orange carbocyanine dye DiI (acceptor) both physically encapsulated in the core of the SCMs. The third system comprised of a green dye FITC (donor) and rhodamine B (acceptor) both covalently conjugated to the telodendrimer units of the nanoparticles. A dramatic decrease in FRET signal for the non-crosslinked micelles occurred within 30 min in the presence of human plasma indicated that human plasma can disrupt the non-cross-linked nanoparticles. It was also observed that all the four major groups of lipoprotein particles (chylomicron, HDL, LDL and VLDL) cause a rapid decrease of FRET efficiency of FRET-NCMN1 while serum albumin (HSA) and immunoglobulin gamma (IgG, the most abundant antibody in blood) have minimal effect on the FRET efficiency. The FRET ratio of the disulfide crosslinked micelles decreased much slower than that of non-crosslinked using the same FRET pair in the presence of HDL, LDL and VLDL indicating the disulfide crosslinked micelles have better stability and less premature drug release. However, the FRET signal of the disulfide crosslinked micelles dropped dramatically in the presence of human plasma and reducing agents (glutathione (GSH) and N-acetylcysteine (NAC)), indicating their reduction sensitivity. Furthermore, the disulfide crosslinked micelles were demonstrated to have significantly increased stability in animal models in comparison with their parent non-crosslinked micelles utilizing FRET technique [25].

The FRET technique has also been utilized to characterize the above mentioned reversible boronate crosslinked micelles [43]. We have used DiO and rhodamine B as a FRET pair to investigate the stability of NCM and BCM4. The efficient energy transfer from DiO to rhodamine B upon excitation of DiO at 480 nm indicated that the proximity between DiO and rhodamine B was within the FRET range. In the *in vivo* FRET studies, the FRET ratio of NCM decreased rapidly to 46% within 1 min post-injection and dropped to 21% 24 min after injection into nude mice via tail vein. However, the FRET ratio of BCM4 decreased much slower than that of NCM at the same micelle concentration, indicating the boronate crosslinking greatly enhanced the *in vivo* stability of the micelles, therefore, will decrease premature payload release.

As demonstrated above, SCMs are able to minimize the interaction of micellar nanoparticles with blood proteins (e.g. lipoproteins), improve the stability of micelles in the blood, prevent premature drug release, and enhance the delivery of drug to the tumor sites.

3. Pharmacokinetics and biodistribution of SCMs

Recently, stimuli-responsive cross-linked micelles have shown several attractive and distinct advantages compared to the non-cross-linked micelles. Ideally, the crosslinking could minimize the interactions between micelles and blood components such as plasma proteins

and lipoproteins and prevent the micelles from premature dissociation upon extreme dilution in blood stream. Therefore, SCMs may have prolonged blood circulation time and eventually deliver more drugs into tumor tissue or tumor cells. In order to optimize the regimen for clinical applications, it is very important to monitor the pharmacokinetics (PK) and biodistribution of SCMs *in vivo*. Several approaches such as radio-labeling or fluorescent-labeling of polymer carriers and/or drug payloads are the most efficient way so far to determine the *in vivo* fate of polymeric micelles.

A type of pH-responsive core cross-linked micelles also termed “polyion core micelles” synthesized by PEO-b-PMA block copolymers exhibit unique pharmacokinetics and biodistribution [72, 73]. The core of the micelles comprises a network of the cross-linked polyanions formed by poly(methacrylic acid) with Ca^{2+}, which is surrounded by the hydrophilic PEO shell. To examine accumulation of CDDP-loaded micelles in cancer cells, the total Pt(II) content was measured in human ovarian carcinoma A2780 cells following their exposure to 50 μM free CDDP or CDDP-loaded micelles (with 20% degree of crosslinking) by ICP-MS. The net accumulation of Pt(II) was substantially higher in cells treated with CDDP-loaded and crosslinked micelles compared to cells treated with the free drug. These data demonstrated that the pH-responsive cross-linked micelles have an increased chemical stability, unique responsive drug release and accumulation in tumor site.

Another type of core-crosslinked (CCL) micelles based on mPEG5000 and N-(2-hydroxyethyl)methacrylamide)-oligolactates (mPEG-b-p(HEMAm-Lacn)) was labelled with ^{3}H to investigate its circulation kinetics and biodistribution in ^{14}C (head and neck squamous-cell carcinoma line)-tumor bearing mice [26]. The non-crosslinked (NCL) micelles were rapidly eliminated from the circulation with only 6% of the injected dose (ID) present after 4 h whereas CCL micelles exhibited prolonged circulation times and more than 50% ID still present in the systemic circulation after 6 h. Hence, the area under curve (0–24 h) of CCL was substantially larger than that of NCL micelles (990 versus 136% ID×h/mL blood). Although NCMs exhibited some initial tumor uptake at 4 h post-injection (2.5% ID), only 1.1% ID/g was recovered in the tumors after 24 h. In contrast, CCL micelles showed almost 6 times higher uptake in the tumors with more than 2-fold lower accumulation in the liver than NCMs at 24 h post-injection. More importantly, CCL micelles still remained a considerable tumor accumulation after 48 h (5.8% ID/g) by when the blood levels of ^{3}H-labelled CCL micelles were negligible. Therefore, the CCL micelles indicated prolonged circulation, better extravasation and tumor retention compared with the NCL micelles.

The *in vivo* blood elimination of the reversible boronate crosslinked micelles (BCMs) labeled with rhodamine was also monitored in our previous study [43]. After intravenous injection, the rhodamine B signal of non-crosslinked micelles decreased into background level with 10 hr post injection, whereas the signal of BCMs was 6 times higher at 10 hr and lasted for more than 24 hr. These data demonstrated BCMs exhibited slower elimination during the blood circulation than the corresponding non-crosslinked micelles, which may significantly improve the pharmacokinetic profile of conventional water-insoluble anticancer drugs.

We have also investigated the blood elimination profiles and biodistribution of disulfide crosslinked micelles (DCMs) in comparison with the corresponding non-crosslinked micelles (NCMs) [44]. Two separate types of near infra-red fluorescent (NIRF) dye-labeled NCMs and DCMs were developed to track the *in vivo* fate of the carriers and drug. BODIPY 650/665, an organic near infrared dye, was conjugated to nanocarriers and DiD, a hydrophobic near infra-red dye, was physically encapsulated into the core of the micelles as a drug surrogate. The signal of BODIPY 650/665 and DiD in NCMs was found to decrease faster than that of DCMs by monitoring the fluorescence intensity of BODIPY or DiD in the

blood samples collected from tumor free nude mice at different time points post intravenous injection. BODIPY signal of DCMs in blood was up to 8 times higher than that of NCMs within 8 h post-injection and sustained up to 24 h. A similar trend of circulation kinetics was observed for the DiD-loaded NCMs and DCMs (Fig. 10A). The results indicated that DCMs have had longer blood circulation time than NCMs. Furthermore, in the *in vivo* NIRF optical imaging studies in SKOV-3 ovarian cancer xenograft mouse model, DiD-loaded DCMs were found to preferentially accumulate in the tumor site. A significant difference of fluorescence signal between tumor and background occurred at 4 h after administration and sustained up to 72 h. *Ex* vivo imaging at 72 h post-injection further confirmed the preferential uptake of DCMs in tumor compared to normal organs (Fig. 10B).

To summarize, the few studies published so far on pharmacokinetics and biodistribution demonstrate that stimuli-responsive crosslinking of micelles is able to significantly improve their stability in the blood, prolong their blood circulation, and enhance their tumor accumulation. After reaching the tumor site, SCMs are able to structurally respond to tumor micro-environments, such as low pH, and reductive condition, resulting in fast release of drug payload locally in the tumor tissue or inside the cancer cells.

4. Preclinical efficacy of SCMs

The physico-chemical property, pharmacokinetics and biodistribution of SCMs have been introduced in the previous section. Ultimately, the SCMs should be able to efficiently kill cancer cells *in vitro* and significantly inhibit the tumor growth *in vivo*. In the present section, we will discuss the *in vitro* and *in vivo* anti-cancer therapeutic efficacy of drug-loaded SCMs.

4.1 *In vitro* anti-tumor activity—As described in the previous section, a novel class of reversible stimuli-responsive disulfide cross-linked micelle was exploited by our laboratory based on thiolated telodendrimers [44]. The disulifide crosslinked micelles (DCMs) had a higher PTX-loading efficiency and slower drug release profile than the non-crosslinked counterpart, however, the drug release rate from PTX-DCMs could be gradually facilitated by GSH at the intracellular concentration. The intracellular uptake of DiD fluorescent labeled DCMs in SKOV-3 ovarian cancer cells was observed under the confocal microscopy. As shown in the Fig. 11A, the DiD fluorescence intensity increased gradually during the first 3 h of incubation, and the internalized DCMs were found to localize mainly in the cytoplasmic region. The cell viability of blank and PTX-loaded DCMs were measure by MTT assay. Blank NCMs and DCMs exhibited no significant cytotoxicity against SKOV-3 ovarian cancer cells at the concentration up to 1.0 mg/mL. When loaded with PTX, PTX-NCMs had comparable *in vitro* cytotoxicity against SKOV-3 ovarian cells with Taxol®, whereas PTX-DCMs showed lower anti-cancer activity than both PTX-NCMs and Taxol®, which was likely due to the slower drug release profile from PTX-DCMs (Fig. 11B). However, PTX-DCMs exhibited enhanced cytotoxicity when glutathione monoethyl ester (GSH-OEt) was introduced to enhance intracellular GSH concentration which facilitated intracellular drug release due to the cleavage of intramicellar disulfide bridges of DCMs (Fig. 11C).

The anti-tumor activity of the PTX-loaded reversibly boronate cross-linked micelles (PTX-BCM4) were also evaluated in comparison with PTX-loaded non-crosslinked micelles and free Taxol® [43]. They were incubated with SKOV-3 ovarian cancer cell for 1 h followed by PBS washing and then 23 h further incubation. PTX-NCMs and Taxol® showed similar anti-cancer activity, whereas PTX-BCM4 exhibited considerably lower cytotoxicity at equal PTX dose levels (Fig. 11D). Under the tissue culture medium condition of pH 7.4, 5.5 mM glucose and 10% fetal calf serum (containing lipoproteins), BCM4 remained stable and level

of drug release was limited. However, under acidic environment and in the presence of mannitol, drug released from BCM4 accelerated and therefore cytotoxicity was found to match that of PTX-NCMs and Taxol® (Fig. 11D). This result is consistent with previous discussion that acidic pH and mannitol can lead to the disintegration of the cross-linking boronates of BCM4 facilitating the release of drug from the nanoparticles.

4.2 *In vivo* therapeutic efficacy—SCMs have been widely studied because of their prolonged circulation time, good stability, high drug-loading capacity and on-demand drug release under certain stimulating environment. SCMs are expected to serve as a promising nanoparticle drug delivery system. Surprisingly, there are only a few reports in the literatures that have demonstrated the *in vivo* anti-tumor efficacy of SCMs.

For example, the *in vivo* anti-tumor efficacy of pH and redox dual-sensitive interfacially crosslinked micelles based on (mPEG-PAsp(MEA)-PAsp(DIP)) triblock copolymers prepared by Shuai et al. was evaluated in nude mice bearing the Bel-7402 tumor. The crosslinked micelle formulation of DOX was demonstrated to be more efficacious than free DOX [62]. The crosslinked mPEG-b-p(HPMAm-Lacn) micelles with covalently entrapped doxorubicin developed by Talelli et al. also showed better anti-tumor activity than free DOX in mice bearing B16F10 melanoma carcinoma [46].

The anti-cancer efficacy and toxicity profiles of our previously developed reversible disulfide crosslinked micelles loaded with PTX and VCR were evaluated in ovarian cancer and B-cell lymphoma mouse models, respectively [44, 55]. Subcutaneous SKOV-3 tumor xenograft bearing mice was chosen in the therapeutic efficacy study of disulfide cross-linked micelles (DCM) in comparison with the non-crosslinked micelles (NCM) and paclitaxel (Taxol®). Compared to the control group, all the three treatment groups (clinical formulation of Taxol®, PTX-DCMs and PTX-NCMs) at 10 mg PTX/kg showed significant tumor growth inhibition ($p<0.05$) (Fig. 12A) and prolonged survival time, (Fig. 12B). However, the tumor growth rate of mice in the PTX-DCMs groups was much lower than that in the PTX-NCMs group at both 10 mg PTX/kg and 30 mg PTX/kg dose. This can easily be explained by the lower premature drug release in the PTX-DCMs group. We have also tested the combination of PTX-DCMs with NAC (a reducing agent approved by FDA as a mucolytic agent and for the management of acetaminophen (Tylenol) overdose) given 24 h after each given dose of PTX-DCMs. NAC was given on-demand to facilitate drug release at the tumor site. Importantly, this treatment arm is the most efficacious to inhibite tumor growth (Fig. 12C). No palpable tumors were detected in 6 of the 8 mice by the end of the therapeutic studies. The result provides the preclinical “proof-of-concept” that exogenous agent such as NAC can be used for on-demand drug release of SCMs in cancer therapy.

In our another study, stimuli-responsive disulfide cross-linked micelles were applied for the targeted delivery of vincristine (VCR) to B-cell lymphoma *in vivo* [55]. VCR encapsulated disulfide cross-linked micelles with a size of about 16 nm were formed by PEG^{5k}-Cys4-L_8-CA_8 telodendrimers. Non-Hodgkin lymphoma xenograft bearing mice were treated with PBS, conventional VCR (1 mg/kg), DCM-VCR (1 mg/kg) with or without 100 mg/kg NAC given 24 h after the nanotherapeutic dose, or high dose DCM-VCR (2.5 mg/kg) groups. Significant inhibition in tumor growth was observed for all VCR treatment groups compared with the PBS controlled group ($p<0.05$). The mice treated with 1 mg/kg DCM-VCR showed a significantly less weight lost than those treated with free VCR (1 mg/kg). Furthermore, 1 mg/kg DCM-VCR followed by 100 mg/kg NAC 24 h later showed superior anti-tumor effect to the free VCR group. High dose (2.5 mg/kg) of DCM-VCR exhibited even better tumor growth inhibition, and more importantly, it was well tolerated, with an equivalent amount of weight lost as the 1 mg/kg conventional VCR group.

Thus far, the number of papers reporting *in vivo* therapeutic studies of SCMs is rather limited; however, the results are convincingly unanimous in showing that SCMs are able to deliver anti-cancer drugs to tumor tissue more efficiently, and enhance anti-cancer therapeutic efficacy in preclinical animal models, when compared to non-crosslinked micelles.

5. Conclusion and Future Outlook

The research on SCMs addresses a critical issue in cancer research to reduce drug adverse toxicities and increase drug efficacy. State-of-the-art design of SCMs with enhanced stability and stimuli sensitivity represents the frontier development of nanomedicine. It is a convenient and efficacious approach to prevent pre-mature drug release during circulation and deliver high concentration of drug to tumor sites on-demand. It shows great promise in formulating many existing and new drugs to enhance their therapeutic efficacies and lower their side-effects against cancers and other diseases.

Athough the main focus of the nanodelivery field has been in cancer imaging and therapy, one ought not ignor its applications in the treatment of many benign diseases. With the appropriate targeting ligands, one may be able to deliver nanotherapeutics to target tissues of interest, such as liver, lung, adrenal glands, bone, stroke sites, ischemic myocardium, and brain endothelial cells. Recent work in our laboratory demonstrated that dexamethasone-loaded in nanomicelles is more efficacious than free dexamethasone in the treatment of experimentally induced asthma in murine model. Ligands that can facilitate the crossing of the blood-brain-barrier may allow one to deliver SCMs to the brain tissues efficiently, bypassing the need to give intra-thecal drugs. SCMs encapsulated with potent antibiotics and decorated with specific ligands against cell surface proteins of microbes and parasites may revolutionalize the treatment of many globally important infectious diseases. Ligands that recognize host cells such as monocytes and macrophages may allow delivery of potent antibiotics for the treatment and eradication of mycobacteria from the patients. In order to realize the promise of using small RNAs for the treatment of many diseases, one needs to develop an efficient delivery system. We believe nanocarrier equipped with appropriate targeting ligands and endosomal releasing molecules is the likely solution.

To translate SCMs into efficacious therapies in the clinic will require more than just stable formulation with minimal drug release during the circulation [74]. The other following important factors will also need to be considered: 1) the nanocarrier itself needs to be biodegradable, biocompatible, and nontoxic; 2) scale-up production of the nanoparticle drugs needs to be economical, reproducible and robust; 3) formulation procedures by the pharmacist at the clinic needs to be simple and reproducible; 4) the shelf-life of the nanoformulation needs to be measured in months; 5) the particle size distribution needs to be narrow; 5) the uptake by the reticuloendothelial system in the liver, spleen, lung and bone marrow needs to be minimal; 6) To be fully effective, the nanoparticle drugs needs to delivered intracellularly, which can be achieved by decorating nanocarriers with cancer cell targeting ligands that facilitate receptor-mediated endocytosis. Future effort should be focused on the development of nanocarriers that fulfill all the above mentioned criteria.

Taken all together, a bright future may be foreseen for nanoparticle drug delivery system, especially for stimuli-responsive crosslinked and cancer specific targeting nanocarriers. Many drugs that had failed previously because of formulation issues or toxicity issues may possibly be resurrected by incorporating and adopting the stimuli-responsive crosslinked nanocarriers technology for efficient delivery.

Acknowledgments

The authors thank the financial support from NIH/NCI (R01CA115483 to K.S.L.), NIH/NIBIB (R01EB012569 to K.S.L.), Prostate Cancer Foundation Creative Award (to K.S.L.), US Department of Defense (DoD) PCRP Award (W81XWH-12-1-0087 to Y.L.) and DoD BCRP Award (W81XWH-10-1-0817 to K.X.).

List of all abbreviations

EPR	Electron paramagnetic resonance
FRET	Fluorescence resonance energy transfer
MDR	Multidrug resistance
CMC	Critical micelle concentration
HDL	High density lipoprotein
LDL	Low density lipoprotein
VLDL	Very low density lipoprotein
DCMs	Disulide crosslinked micelles
NCMs	Non-crosslinked micelles
BCMs	Boronate crosslinked micelles
EPR	Enhanced permeability and retention
PTX	Paclitaxel
DOX	Doxorubicin
VCR	Vincristine
MTX	Methotrexate
GSH	Glutathione
RAFT	Reversible addition-fragmentation chain transfer
PEG-*b*-PHPMA-LA	Poly(ethylene glycol)-*b*-poly(*N*-2-hydroxypropyl methacrylamide)-lipoic acid
DTT	Dithiothreitol
LA	Lipoic acids
SDS	Sodium dodecyl sulfate
BIC	Block ionomer complexes
PEO-*b*-PMA	Poly(ethylene oxide)-*b*-poly(methacylic acid)
HEC-*g*-PAA	Cellulose-*g*-poly(acrylic acid)
PHEA*b*-PBA	Poly(hydroxyethyl acrylate)-*block*-poly(*n*-butyl acrylate)
PEG-*b*-PDEA-*s*-TMSPMA	Poly(ethylene glycol)-*b*-poly((2-(diethylamino) ethyl methacrylate)-*s*-(3-(trimethoxysilyl) propyl methacrylate))
PLA	Polylactate
PCL	*Polycaprolactone*
mPEG-b-pHPMA$_m$-Lac$_n$	Poly(ethylene glycol)-b-poly[N-(2-hydroxypropyl) methacrylamide-lactate]

DOX-MA	DOX methacrylamide derivative
PEG-PAsp-PPhe	Poly(ethylene glycol)-poly(L-aspartic acid)-poly(L-phenylalanine)
DLS	Dynamic light scattering
KSV	Stern-Volmer quenching constant
PEG-b-PLys-b-PPha	Poly(ethylene glycol)-b-poly(L-lysine)-b-poly(L-phenylalanine)
DTSSP	3,3'-dithiobis(sulfosuccinimidylpropionate)
TCEP	Tris(2-carboxyethyl)phosphine
mPEO-PAPMA-PDPAEMA	Methoxy poly(ethylene oxide)-*b*-poly(*N*-(3-aminopropyl) methacrylamide)-poly(2-(diisopropylamino)ethyl methacrylate)
DTBP	Dimethyl 3,3-dithiobispropionimidate
PAEMA	Poly(2-aminoethylmethacrylamide)
NIPAM	*N*-isopropylacrylamide
DSDMA	Bis(2-methacryloyloxyethyl) disulfide
ATRP	Atom transfer radical polymerization
SCRM	Shell cross-linked reverse micelles
DMAEMA	Dimethylaminoethyl methacrylate

References

1. Lansiaux A. Nanotechnologies and cancer: diagnosis and therapeutic future. Bull. Cancer. 2008; 95:391–391.
2. Lue N, Ganta S, Hammer DX, Mujat M, Stevens AE, Harrison L, Ferguson RD, Rosen D, Amiji M, Iftimia N. Preliminary evaluation of a nanotechnology-based approach for the more effective diagnosis of colon cancers. Nanomedicine. 2010; 5:1467–1479. [PubMed: 21128727]
3. Koo H, Lee H, Lee S, Min KH, Kim MS, Lee DS, Choi Y, Kwon IC, Kim K, Jeong SY. In vivo tumor diagnosis and photodynamic therapy via tumoral pH-responsive polymeric micelles. Chem Commun (Camb). 2010; 46:5668–5670. [PubMed: 20623050]
4. Nanoparticle 'fingerprinting' technique could improve cancer diagnosis. Bioanalysis. 2009; 1:270–270.
5. Iwakuma N, Toh U, Grobmyer SR, Koura K, Takenaka M, Otsuka H, Takahashi R, Shirouzu K. The Potential of Targeting Nanoparticle for Breast Cancer Diagnosis. European Journal Of Cancer. 2012; 48:S62–S62.
6. Gomes-da-Silva LC, Santos AO, Bimbo LM, Moura V, Ramalho JS, de Lima MCP, Simoes S, Moreira JN. Toward a siRNA-containing nanoparticle targeted to breast cancer cells and the tumor microenvironment. International Journal Of Pharmaceutics. 2012; 434:9–19. [PubMed: 22617794]
7. Choi WI, Kim JY, Heo SU, Jeong YY, Kim YH, Tae G. The effect of mechanical properties of iron oxide nanoparticle-loaded functional nano-carrier on tumor targeting and imaging. Journal Of Controlled Release. 2012; 162:267–275. [PubMed: 22824783]
8. Karra N, Benita S. The Ligand Nanoparticle Conjugation Approach for Targeted Cancer Therapy. Current Drug Metabolism. 2012; 13:22–41. [PubMed: 21892918]
9. Ullal AV, Reiner T, Yang KS, Gorbatov R, Min C, Issadore D, Lee H, Weissleder R. Nanoparticle-Mediated Measurement of Target-Drug Binding in Cancer Cells. ACS Nano. 2011; 5:9216–9224. [PubMed: 21962084]
10. Bahadur KCR, Thapa B, Xu PS. pH and Redox Dual Responsive Nanoparticle for Nuclear Targeted Drug Delivery. Mol Pharm. 2012; 9:2719–2729. [PubMed: 22876763]

11. Qiao GM, Gao Y, Li N, Yu ZZ, Zhuo LH, Tang B. Simultaneous Detection of Intracellular Tumor mRNA with Bi-Color Imaging Based on a Gold Nanoparticle/Molecular Beacon. Chemistry-a European Journal. 2011; 17:11210–11215.
12. Gao JH, Chen K, Luong R, Bouley DM, Mao H, Qiao TC, Gambhir SS, Cheng Z. A Novel Clinically Translatable Fluorescent Nanoparticle for Targeted Molecular Imaging of Tumors in Living Subjects. Nano Letters. 2012; 12:281–286. [PubMed: 22172022]
13. Oh SJ, Kang J, Maeng I, Suh JS, Huh YM, Haam S, Son JH. Nanoparticle-enabled terahertz imaging for cancer diagnosis. Optics Express. 2009; 17:3469–3475. [PubMed: 19259185]
14. Saravanakumar G, Kim K, Park JH, Rhee K, Kwon IC. Current Status of Nanoparticle-Based Imaging Agents for Early Diagnosis of Cancer and Atherosclerosis. Journal Of Biomedical Nanotechnology. 2009; 5:20–35. [PubMed: 20055103]
15. Ding H, Wang XJ, Zhang S, Liu XL. Applications of polymeric micelles with tumor targeted in chemotherapy. Journal Of Nanoparticle Research. 2012; 14
16. Singh AK, Hahn MA, Gutwein LG, Rule MC, Knapik JA, Moudgil BM, Grobmyer SR, Brown SC. Multi-dye theranostic nanoparticle platform for bioimaging and cancer therapy. International Journal Of Nanomedicine. 2012; 7:2739–2750. [PubMed: 22701319]
17. Woo HN, Chung HK, Ju EJ, Jung J, Kang HW, Lee SW, Seo MH, Lee JS, Lee JS, Park HJ, Song SY, Jeong SY, Choi EK. Preclinical evaluation of injectable sirolimus formulated with polymeric nanoparticle for cancer therapy. International Journal Of Nanomedicine. 2012; 7:2197–2208. [PubMed: 22619555]
18. Cheng YY, Zhao LB, Li YW, Xu TW. Design of biocompatible dendrimers for cancer diagnosis and therapy: current status and future perspectives. Chemical Society Reviews. 2011; 40:2673–2703. [PubMed: 21286593]
19. Yoon SM, Myung SJ, Kim IW, Do EJ, Ye BD, Ryu JH, Park K, Kim K, Kwon IC, Kim MJ, Moon DH, Yang DH, Kim KJ, Byeon JS, Yang SK, Kim JH. Application of Near-Infrared Fluorescence Imaging Using a Polymeric Nanoparticle-Based Probe for the Diagnosis and Therapeutic Monitoring of Colon Cancer. Digestive Diseases And Sciences. 2011; 56:3005–3013. [PubMed: 21465144]
20. Kong XG, Liu XM, Sun YJ, Yu Y, Zhang YL. Aoe. Multifunctional Nanoparticle with Diagnosis and Therapeutics for Tumour. 2009
21. Nie S, Xing Y, Kim GJ, Simons JW. Nanotechnology applications in cancer. Annu Rev Biomed Eng. 2007; 9:257–288. [PubMed: 17439359]
22. Gao ZG, Lukyanov AN, Singhal A, Torchilin VP. Diacyllipid-polymer micelles as nanocarriers for poorly soluble anticancer drugs. Nano Letters. 2002; 2:979–982.
23. Davis ME, Chen ZG, Shin DM. Nanoparticle therapeutics: an emerging treatment modality for cancer. Nat Rev Drug Discov. 2008; 7:771–782. [PubMed: 18758474]
24. Manzoor AA, Lindner LH, Landon CD, Park JY, Simnick AJ, Dreher MR, Das S, Hanna G, Park W, Chilkoti A, Koning GA, ten Hagen TLM, Needham D, Dewhirst MW. Overcoming Limitations in Nanoparticle Drug Delivery: Triggered, Intravascular Release to Improve Drug Penetration into Tumors. Cancer Res. 2012; 72:5566–5575. [PubMed: 22952218]
25. Li Y, Budamagunta MS, Luo J, Xiao W, Voss JC, Lam KS. Probing of the assembly structure and dynamics within nanoparticles during interaction with blood proteins. ACS nano. 2012; 6:9485–9495. [PubMed: 23106540]
26. Rijcken CJ, Snel CJ, Schiffelers RM, van Nostrum CF, Hennink WE. Hydrolysable corecrosslinked thermosensitive polymeric micelles: synthesis, characterisation and in vivo studies. Biomaterials. 2007; 28:5581–5593. [PubMed: 17915312]
27. Jackson AW, Fulton DA. Making polymeric nanoparticles stimuli-responsive with dynamic covalent bonds. Polymer Chemistry. 2013; 4:31–45.
28. Huang YC, Yang YS, Lai TY, Jan JS. Lysine-block-tyrosine block copolypeptides: Self-assembly, cross-linking, and conjugation of targeted ligand for drug encapsulation. Polymer. 2012; 53:913–922.
29. Li YL, Zhu L, Liu ZZ, Cheng R, Meng FH, Cui JH, Ji SJ, Zhong ZY. Reversibly Stabilized Multifunctional Dextran Nanoparticles Efficiently Deliver Doxorubicin into the Nuclei of Cancer Cells. Angew Chem Int Edit. 2009; 48:9914–9918.

30. Li QM, Zhu LJ, Liu RG, Huang D, Jin X, Che N, Li Z, Qu XZ, Kang HL, Huang Y. Biological stimuli responsive drug carriers based on keratin for triggerable drug delivery. Journal Of Materials Chemistry. 2012; 22:19964–19973.

31. Meng FH, Cheng R, Deng C, Zhong ZY. Intracellular drug release nanosystems. Materials Today. 2012; 15:436–442.

32. Popescu MT, Tsitsilianis C, Papadakis CM, Adelsberger J, Balog S, Busch P, Hadjiantoniou NA, Patrickios CS. Stimuli-Responsive Amphiphilic Polyelectrolyte Heptablock Copolymer Physical Hydrogels: An Unusual pH-Response. Macromolecules. 2012; 45:3523–3530.

33. Wang K, Liu Y, Yi WJ, Li C, Li YY, Zhuo RX, Zhang XZ. Novel shell-cross-linked micelles with detachable PEG corona for glutathione-mediated intracellular drug delivery. Soft Matter. 2013; 9:692–699.

34. Meng F, Zhong Z, Feijen J. Stimuli-responsive polymersomes for programmed drug delivery. Biomacromolecules. 2009; 10:197–209. [PubMed: 19123775]

35. Koo AN, Lee HJ, Kim SE, Chang JH, Park C, Kim C, Park JH, Lee SC. Disulfide-cross-linked PEG-poly(amino acid)s copolymer micelles for glutathione-mediated intracellular drug delivery. Chem Commun (Camb). 2008:6570–6572. [PubMed: 19057782]

36. Barick KC, Singh S, Jadhav NV, Bahadur D, Pandey BN, Hassan PA. pH-Responsive Peptide Mimic Shell Cross-Linked Magnetic Nanocarriers for Combination Therapy. Advanced Functional Materials. 2012; 22:4975–4984.

37. Jackson AW, Fulton DA. Triggering Polymeric Nanoparticle Disassembly through the Simultaneous Application of Two Different Stimuli. Macromolecules. 2012; 45:2699–2708.

38. Liu H, Jiang XZ, Fan J, Wang GH, Liu SY. Aldehyde surface-functionalized shell cross-linked micelles with pH-tunable core swellability and their bioconjugation with lysozyme. Macromolecules. 2007; 40:9074–9083.

39. Qi K, Ma QG, Remsen EE, Clark CG, Wooley KL. Determination of the bioavailability of biotin conjugated onto shell cross-linked (SCK) nanoparticles. Journal of the American Chemical Society. 2004; 126:6599–6607. [PubMed: 15161288]

40. Chan Y, Wong T, Byrne F, Kavallaris M, Bulmus V. Acid-labile core cross-linked micelles for pHtriggered release of antitumor drugs. Biomacromolecules. 2008; 9:1826–1836. [PubMed: 18564874]

41. Jiang XZ, Liu SY, Narain R. Degradable Thermo responsive Core Cross-Linked Micelles: Fabrication, Surface Functionalization, and Biorecognition. Langmuir. 2009; 25:13344–13350. [PubMed: 19928937]

42. Harada A, Kataoka K. Supramolecular assemblies of block copolymers in aqueous media as nanocontainers relevant to biological applications. Progress In Polymer Science. 2006; 31:949–982.

43. Li Y, Xiao W, Xiao K, Berti L, Luo J, Tseng HP, Fung G, Lam KS. Well-defined, reversible boronate crosslinked nanocarriers for targeted drug delivery in response to acidic pH values and cis-diols. Angew Chem Int Ed Engl. 2012; 51:2864–2869. [PubMed: 22253091]

44. Li Y, Xiao K, Luo J, Xiao W, Lee JS, Gonik AM, Kato J, Dong TA, Lam KS. Well-defined, reversible disulfide cross-linked micelles for on-demand paclitaxel delivery. Biomaterials. 2011; 32:6633–6645. [PubMed: 21658763]

45. Sun H, Guo B, Cheng R, Meng F, Liu H, Zhong Z. Biodegradable micelles with sheddable poly(ethylene glycol) shells for triggered intracellular release of doxorubicin. Biomaterials. 2009; 30:6358–6366. [PubMed: 19666191]

46. Talelli M, Iman M, Varkouhi AK, Rijcken CJ, Schiffelers RM, Etrych T, Ulbrich K, van Nostrum CF, Lammers T, Storm G, Hennink WE. Core-crosslinked polymeric micelles with controlled release of covalently entrapped doxorubicin. Biomaterials. 2010; 31:7797–7804. [PubMed: 20673684]

47. Kim JE, Cha EJ, Ahn CH. Reduction-Sensitive Self-Aggregates as a Novel Delivery System. Macromol Chem Phys. 2010; 211:956–961.

48. Xing MMQ, Lu CH, Zhong W. Shell cross-linked and hepatocyte-targeting nanoparticles containing doxorubicin via acid-cleavable linkage. Nanomed-Nanotechnol. 2011; 7:80–87.

49. Talelli M, Iman M, Rijcken CJ, van Nostrum CF, Hennink WE. Targeted core-crosslinked polymeric micelles with controlled release of covalently entrapped doxorubicin. Journal of controlled release : official journal of the Controlled Release Society. 2010; 148:e121–e122. [PubMed: 21529592]
50. Lee SJ, Min KH, Lee HJ, Koo AN, Rim HP, Jeon BJ, Jeong SY, Heo JS, Lee SC. Ketal crosslinked poly(ethylene glycol)-poly(amino acid)s copolymer micelles for efficient intracellular delivery of doxorubicin. Biomacromolecules. 2011; 12:1224–1233. [PubMed: 21344942]
51. Takae S, Miyata K, Oba M, Ishii T, Nishiyama N, Itaka K, Yamasaki Y, Koyama H, Kataoka K. PEG-detachable polyplex micelles based on disulfide-linked block catiomers as bioresponsive nonviral gene vectors. J Am Chem Soc. 2008; 130:6001–6009. [PubMed: 18396871]
52. Black SM, Wolf CR. The role of glutathione-dependent enzymes in drug resistance. Pharmacol Ther. 1991; 51:139–154. [PubMed: 1685247]
53. Kartalou M, Essigmann JM. Mechanisms of resistance to cisplatin. Mutat Res. 2001; 478:23–43. [PubMed: 11406167]
54. Wang YC, Li Y, Sun TM, Xiong MH, Wu J, Yang YY, Wang J. Core-shell-corona micelle stabilized by reversible cross-linkage for intracellular drug delivery. Macromolecular rapid communications. 2010; 31:1201–1206. [PubMed: 21590876]
55. Kato J, Li Y, Xiao K, Lee JS, Luo J, Tuscano JM, O'Donnell RT, Lam KS. Disulfide cross-linked micelles for the targeted delivery of vincristine to B-cell lymphoma. Mol Pharm. 2012; 9:1727–1735. [PubMed: 22530955]
56. Gosselin MA, Guo W, Lee RJ. Efficient gene transfer using reversibly cross-linked low molecular weight polyethylenimine. Bioconjug Chem. 2001; 12:989–994. [PubMed: 11716690]
57. Kakizawa Y, Harada A, Kataoka K. Environment-sensitive stabilization of core-shell structured polyion complex micelle by reversible cross-linking of the core through disulfide bond. J Am Chem Soc. 1999; 121:11247–11248.
58. Matsumoto S, Christie RJ, Nishiyama N, Miyata K, Ishii A, Oba M, Koyama H, Yamasaki Y, Kataoka K. Environment-responsive block copolymer micelles with a disulfide cross-linked core for enhanced siRNA delivery. Biomacromolecules. 2009; 10:119–127. [PubMed: 19061333]
59. Kim JO, Sahay G, Kabanov AV, Bronich TK. Polymeric micelles with ionic cores containing biodegradable cross-links for delivery of chemotherapeutic agents. Biomacromolecules. 2010; 11:919–926. [PubMed: 20307096]
60. Kellum MG, Smith AE, York SK, McCormick CL. Reversible Interpolyelectrolyte Shell Cross-Linked Micelles from pH/Salt-Responsive Diblock Copolymers Synthesized via RAFT in Aqueous Solution. Macromolecules. 2010; 43:7033–7040.
61. Xu XW, Flores JD, McCormick CL. Reversible Imine Shell Cross-Linked Micelles from Aqueous RAFT-Synthesized Thermoresponsive Triblock Copolymers as Potential Nanocarriers for "pH-Triggered" Drug Release. Macromolecules. 2011; 44:1327–1334.
62. Dai J, Lin S, Cheng D, Zou S, Shuai X. Interlayer-crosslinked micelle with partially hydrated core showing reduction and pH dual sensitivity for pinpointed intracellular drug release. Angew Chem Int Ed Engl. 2011; 50:9404–9408. [PubMed: 21898731]
63. Xu XW, Smith AE, McCormick CL. Facile 'One-Pot' Preparation of Reversible, Disulfide-Containing Shell Cross-Linked Micelles from a RAFT-Synthesized, pH-Responsive Triblock Copolymer in Water at Room Temperature. Aust J Chem. 2009; 62:1520–1527.
64. Du J, Armes SP. pH-responsive vesicles based on a hydrolytically self-cross-linkable copolymer. J Am Chem Soc. 2005; 127:12800–12801. [PubMed: 16159264]
65. Chen J, Qiu X, Ouyang J, Kong J, Zhong W, Xing MM. pH and reduction dual-sensitive copolymeric micelles for intracellular doxorubicin delivery. Biomacromolecules. 2011; 12:3601–3611. [PubMed: 21853982]
66. Babin J, Lepage M, Zhao Y. "Decoration" of shell cross-linked reverse polymer micelles using ATRP: A new route to stimuli-responsive nanoparticles. Macromolecules. 2008; 41:1246–1253.
67. Zhang L, Bernard J, Davis TP, Barner-Kowollik C, Stenzel MH. Acid-degradable core-crosslinked micelles prepared from thermosensitive glycopolymers synthesized via RAFT polymerization. Macromolecular rapid communications. 2008; 29:123–129.

68. Springsteen G, Wang BH. A detailed examination of boronic acid-diol complexation. Tetrahedron. 2002; 58:5291–5300.
69. Zhu L, Shabbir SH, Gray M, Lynch VM, Sorey S, Anslyn EV. A structural investigation of the N-B interaction in an o-(N,N-dialkylaminomethyl)arylboronate system. J Am Chem Soc. 2006; 128:1222–1232. [PubMed: 16433539]
70. Qin Y, Sukul V, Pagakos D, Cui CZ, Jakle F. Preparation of organoboron block copolymers via ATRP of silicon and boron-functionalized monomers. Macromolecules. 2005; 38:8987–8990.
71. Roy D, Cambre JN, Sumerlin BS. Sugar-responsive block copolymers by direct RAFT polymerization of unprotected boronic acid monomers. Chem Commun (Camb). 2008:2477–2479. [PubMed: 18491020]
72. Bontha S, Kabanov AV, Bronich TK. Polymer micelles with cross-linked ionic cores for delivery of anticancer drugs. J Control Release. 2006; 114:163–174. [PubMed: 16914223]
73. Oberoi HS, Laquer FC, Marky LA, Kabanov AV, Bronich TK. Core cross-linked block ionomer micelles as pH-responsive carriers for cis-diamminedichloroplatinum(II). Journal Of Controlled Release. 2011; 153:64–72. [PubMed: 21497174]
74. Lee J, Lam KS. Perspectives on clinical translation of smart nanotherapeutics. Ther Deliv. 2012; 3:1359–1362. [PubMed: 23323552]
75. Ranucci E, Suardi MA, Annunziata R, Ferruti P, Chiellini F, Bartoli C. Poly(amidoamine) conjugates with disulfide-linked cholesterol pendants self-assembling into redox-sensitive nanoparticles. Biomacromolecules. 2008; 9:2693–2704. [PubMed: 18781798]
76. Peng Q, Hu C, Cheng J, Zhong ZL, Zhuo RX. Influence of Disulfide Density and Molecular Weight on Disulfide Cross-Linked Polyethylenimine as Gene Vectors. Bioconjug Chem. 2009; 20:340–346. [PubMed: 19191568]
77. Kakizawa Y, Harada A, Kataoka K. Environment-sensitive stabilization of core-shell structured polyion complex micelle by reversible cross-linking of the core through disulfide bond. J Am Chem Soc. 1999; 121:11247–11248.
78. Miyata K, Kakizawa Y, Nishiyama N, Harada A, Yamasaki Y, Koyama H, Kataoka K. Block catiomer polyplexes with regulated densities of charge and disulfide cross-linking directed to enhance gene expression. J Am Chem Soc. 2004; 126:2355–2361. [PubMed: 14982439]
79. Xu Y, Meng F, Cheng R, Zhong Z. Reduction-sensitive reversibly crosslinked biodegradable micelles for triggered release of doxorubicin. Macromolecular bioscience. 2009; 9:1254–1261. [PubMed: 19904724]
80. Oba M, Aoyagi K, Miyata K, Matsumoto Y, Itaka K, Nishiyama N, Yamasaki Y, Koyama H, Kataoka K. Polyplex micelles with cyclic RGD peptide ligands and disulfide cross-links directing to the enhanced transfection via controlled intracellular trafficking. Mol Pharm. 2008; 5:1080–1092. [PubMed: 19434856]
81. Sun J, Chen X, Lu T, Liu S, Tian H, Guo Z, Jing X. Formation of reversible shell cross-linked micelles from the biodegradable amphiphilic diblock copolymer poly(L-cysteine)-block-poly(L-lactide). Langmuir. 2008; 24:10099–10106. [PubMed: 18698858]
82. Du J, Armes SP. pH-responsive vesicles based on a hydrolytically self-cross-linkable copolymer. J Am Chem Soc. 2005; 127:12800–12801. [PubMed: 16159264]
83. Chang C, Wei H, Feng J, Wang ZC, Wu XJ, Wu DQ, Cheng SX, Zhang XZ, Zhuo RX. Temperature and pH Double Responsive Hybrid Cross-Linked Micelles Based on P(NIPAAm-co-MPMA)-b- P(DEA): RAFT Synthesis and "Schizophrenic" Micellization. Macromolecules. 2009; 42:4838–4844.

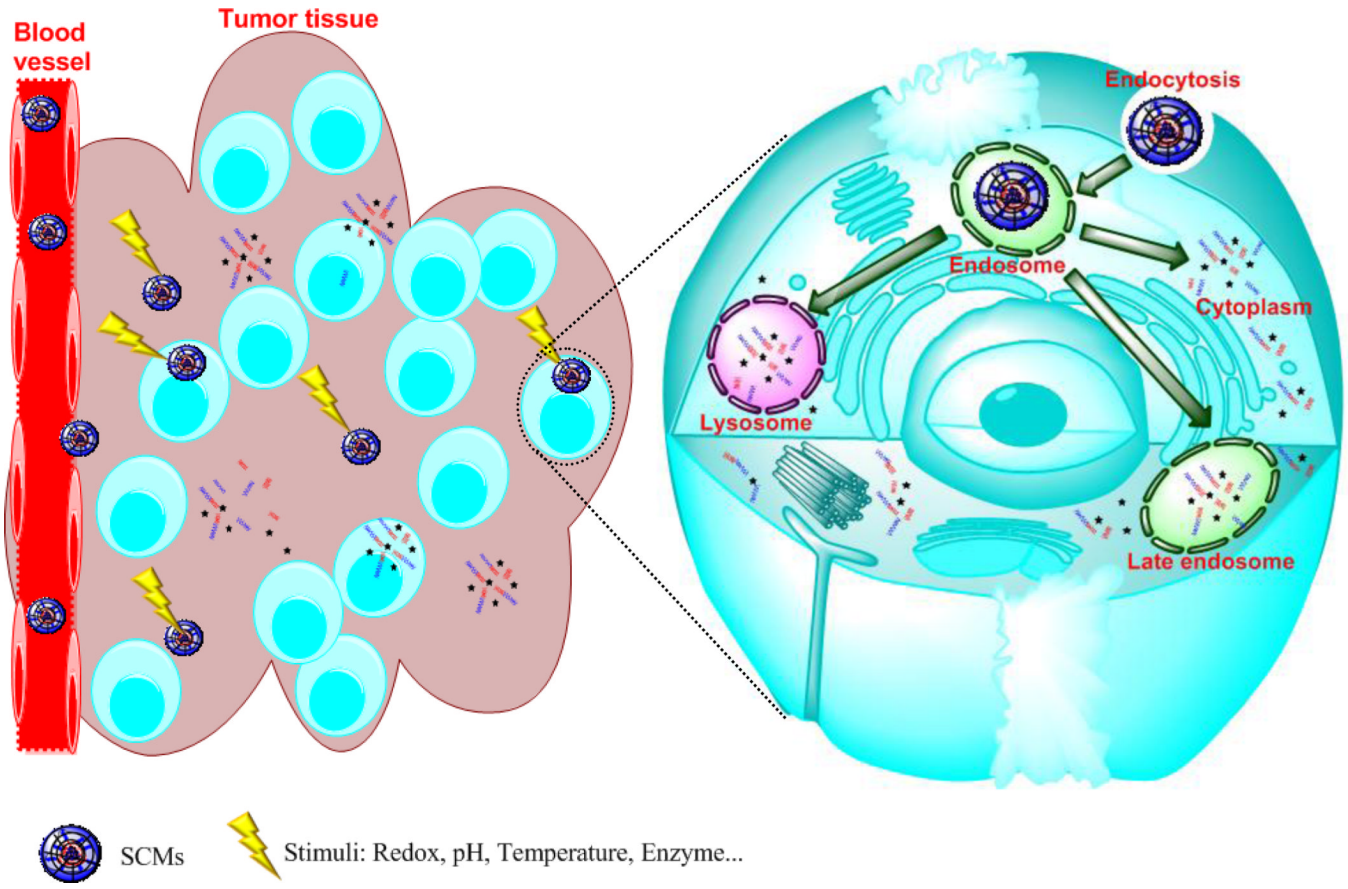

Fig. 1.
Schematic illustration of stimuli-responsive cross-linked micelles (SCMs) for cancer therapy.

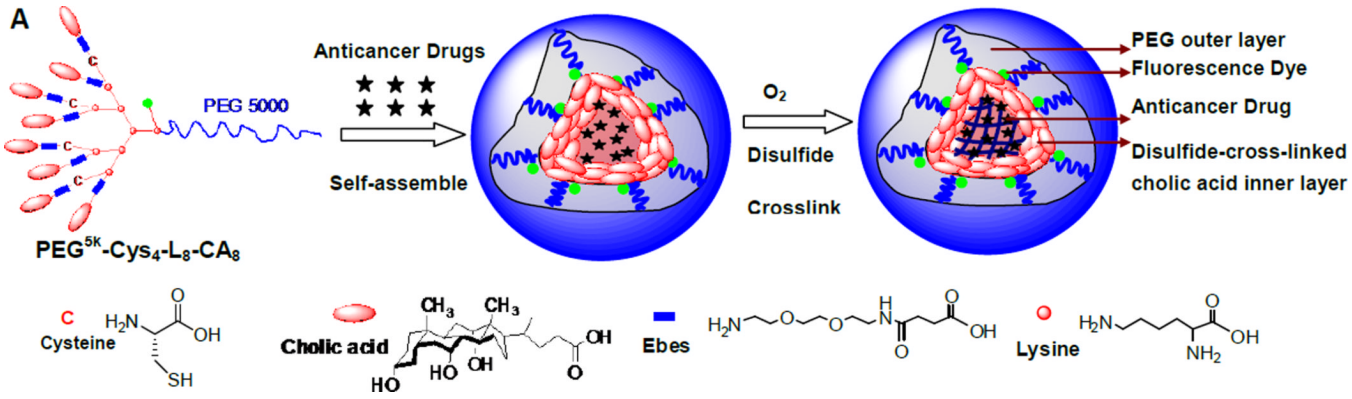

Fig. 2.

Schematic representation of the disulfide cross-linked micelles formed by oxidization of thiolated telodendrimer PEG^{5k}-Cys_4-L_8-CA_8 after self-assemble. Reprinted from [44], Copyright (2011), with permission from Elsevier.

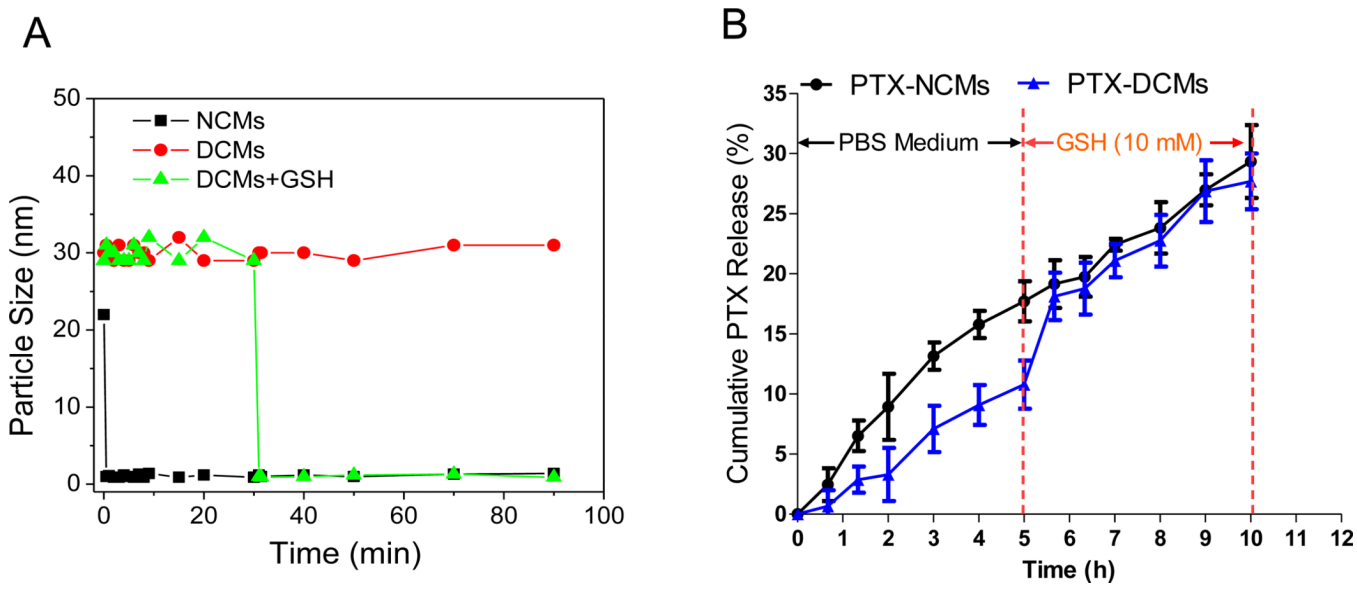

Fig. 3.

(**A**) The stability in particle size of NCMs and DCMs in the presence of 2.5 mg/mL SDS measured by DLS.(**B**) GSH-responsive PTX release profiles of PTX-DCMs by adding GSH (10 mM) at a specific release time (5h) comparing with PTX-NCMs. Reprinted from [44], Copyright (2011), with permission from Elsevier.

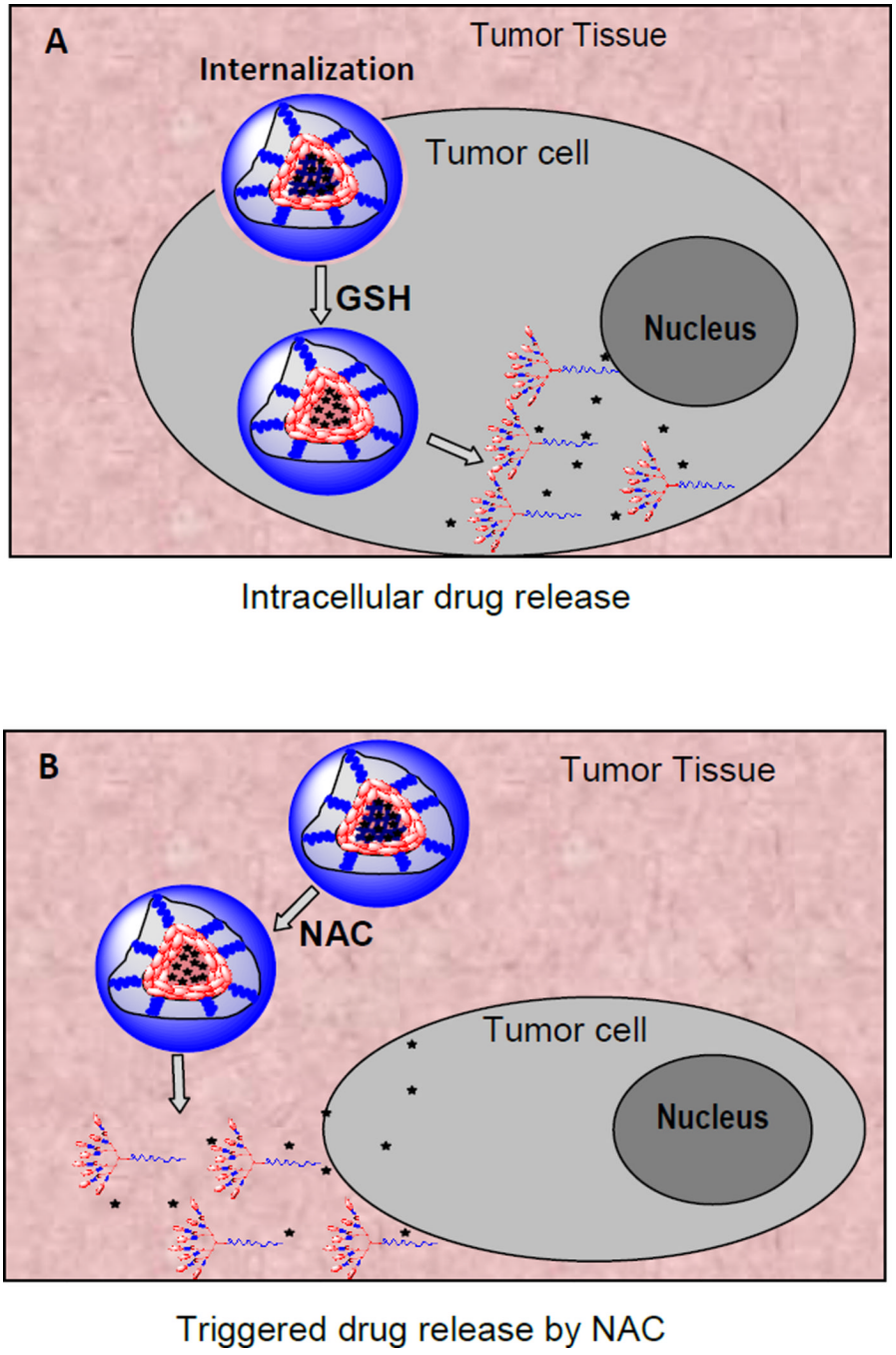

Fig. 4.

Schematic illustration of the hypothesized mechanisms for reducing agents (**A**: GSH, **B**: NAC) mediated drug release once the PTX-DCMs accumulated at tumor sites. Reprinted from [44], Copyright (2011), with permission from Elsevier.

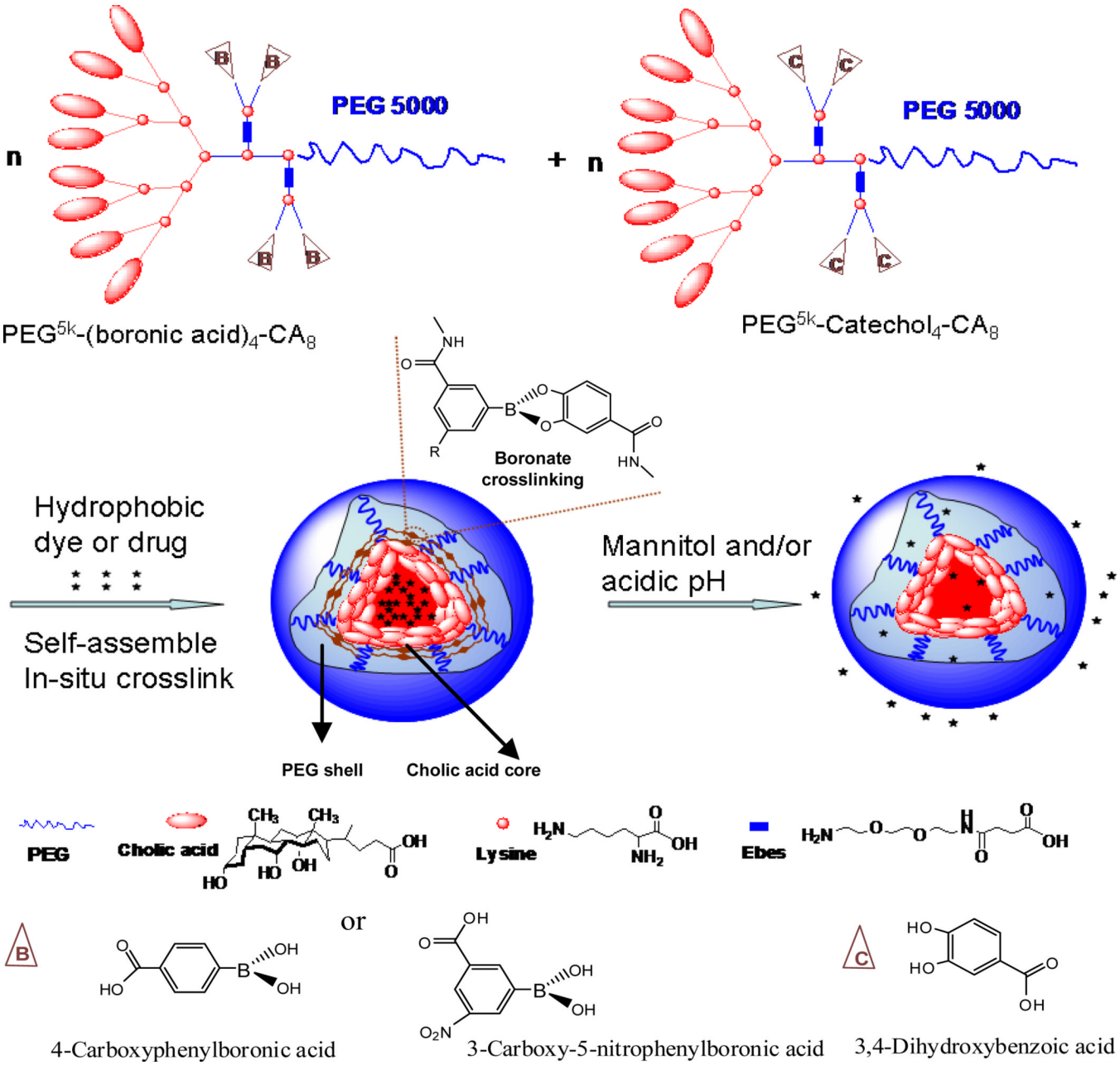

Fig. 5.

Schematic representation of the telodendrimer pair [PEG^{5k}-(boronic acid/catechol)$_4$-CA$_8$] and the resulting boronate crosslinked micelles (BCMs) in response to mannitol and/or acidic pH [43]. Copyright Wiley-VCH Verlag GmbH & Co. KGaA. Reproduced with permission from [43].

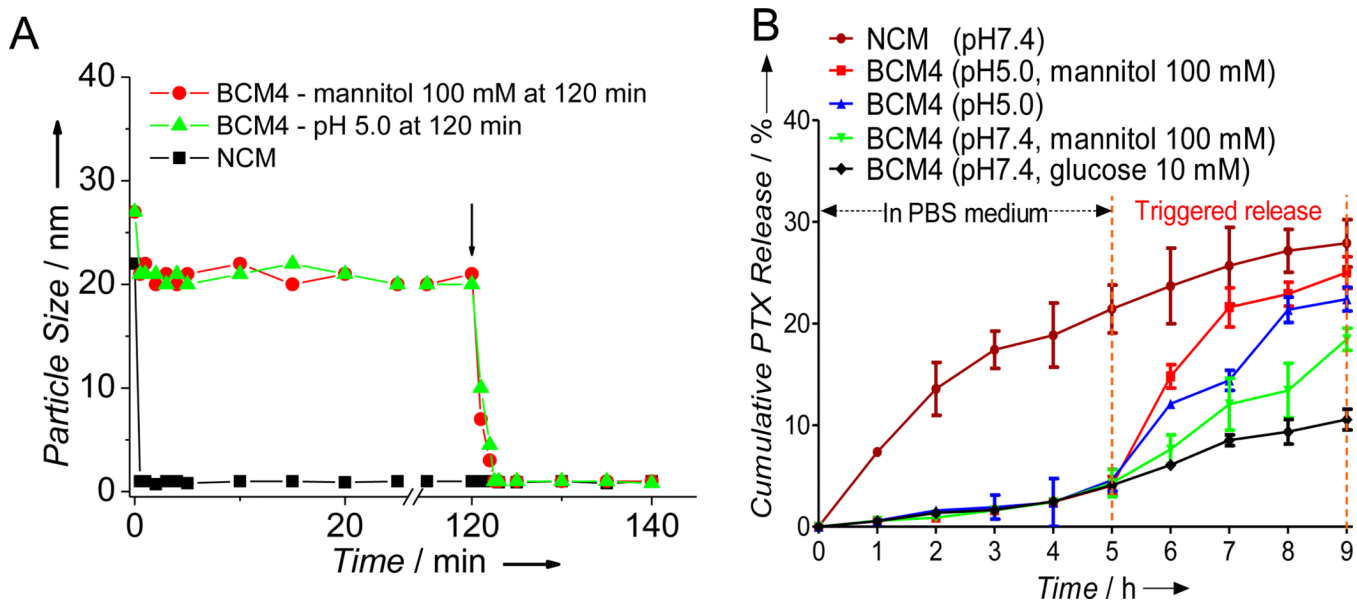

Fig. 6.

(**A**) Continuous dynamic light scattering measurements of NCMs in SDS and BCM4 in SDS for 120 min, at which time mannitol was added or pH of the solution was adjusted to 5.0 (see arrow). (**B**) pH- and diol- responsive PTX release profiles of BCM4 by treating with diols (mannitiol and glucose) and/or pH 5.0 at 5 h compared with that of NCMs [43]. Copyright Wiley-VCH Verlag GmbH & Co. KGaA. Reproduced with permission from [43].

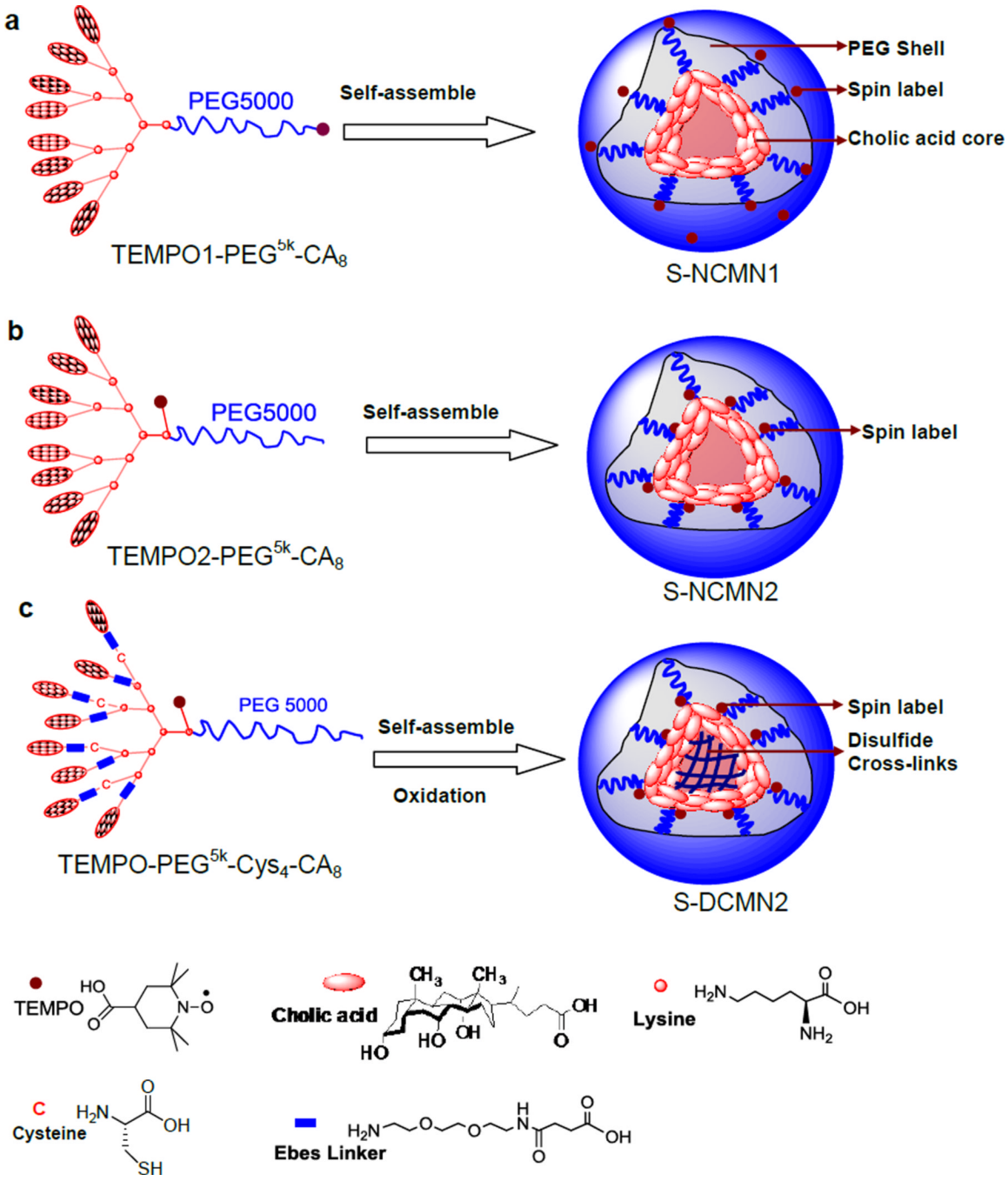

Fig. 7.

Schematic illustration of the spin labelled non-crosslinked nanoparticles by the self-assembly of (**a**) the PEG^{5k}-CA_8 telodendrimer with a spin label attached to the end of the hydrophilic PEG chain and (**b**) the PEG^{5k}-CA_8 telodendrimer with a spin label attached to the lysine side chain at the junction between the linear PEG chain and the dendritic core. (**c**) Schematic illustration of the spin labelled disulfide crosslinked nanoparticles (S-DCMN2) by the self-assembly of the cysteine containing PEG^{5k}-Cys_4-CA_8 telodendrimer with a spin label attached to the lysine side chain at the junction between the linear PEG chain and the

dendritic core followed by oxidation to form disulfide crosslinks [25]. Reprinted with permission from [25]. Copyright (2012) American Chemical Society.

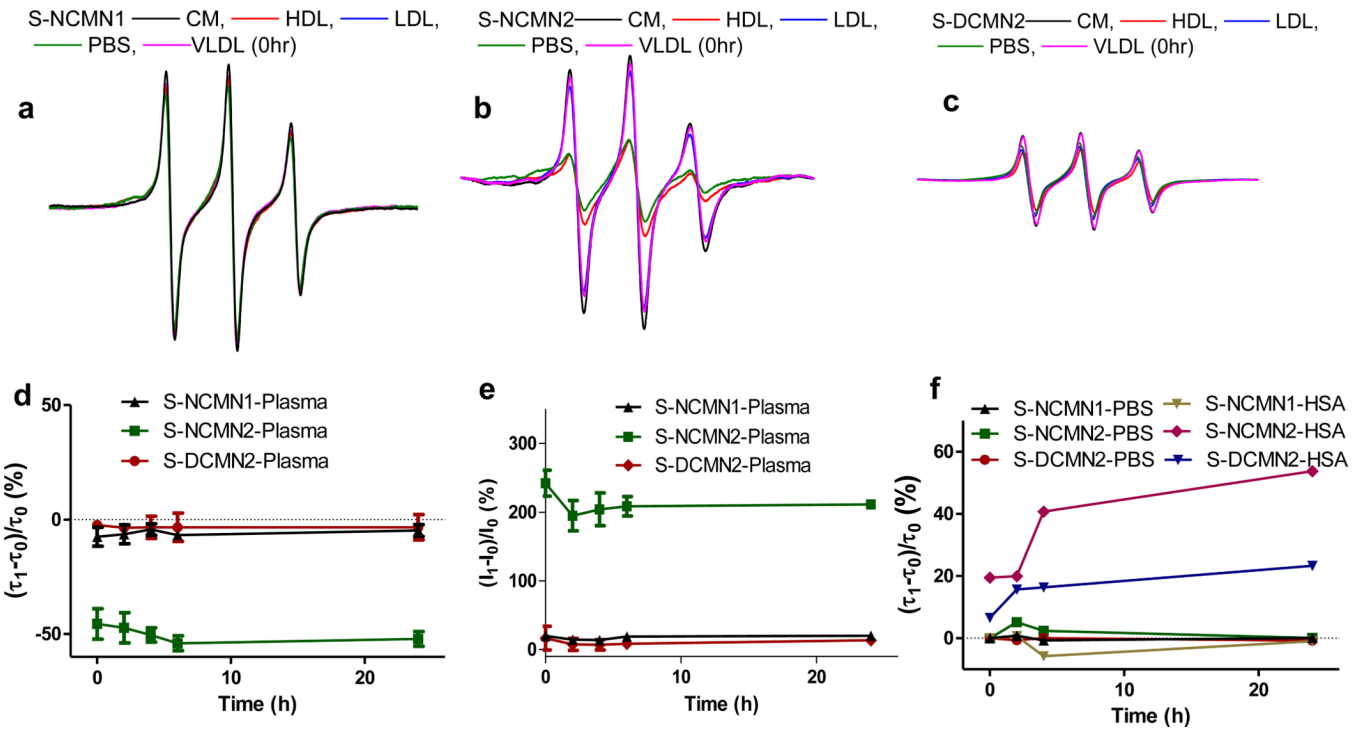

Fig. 8.

Representative time-resolved EPR spectra S-NCMN1 (**a**), S-NCMN2 (**b**) and S-DCMN2 (**c**) in the presence of CM (1.0 mg/mL), HDL (2.0 mg/mL), LDL (2.0 mg/mL), PBS and VLDL (1.0 mg/mL). The percentage changes in rotational correlation time $((\tau_1 - \tau_0)/\tau_0)$ of the three types of spin labelled nanoparticles in human plasma at different time points (**d**), where τ_0 is the rotational correlation time of the sample in PBS while τ_1 is the rotational correlation time of the corresponding peak in a different media under identical instruments conditions, values reported are the mean diameter ± SD for duplicate samples; The percentage of EPR intensity changes $((I_1-I_0)/I_0)$ of the three types of spin labelled nanoparticles in human plasma at different time points (**e**), where I_0 is the intensity of the highest peak in the EPR spectrum of the sample in PBS while I_1 is the intensity of the corresponding peak in a different media under identical instruments conditions, values reported are the mean diameter ± SD for duplicate samples; The $((\tau_1 - \tau_0)/\tau_0)$ value of the three types of spin labelled nanoparticles in PBS and HSA at different time points (**f**) [25]. Reprinted with permission from [25]. Copyright (2012) American Chemical Society.

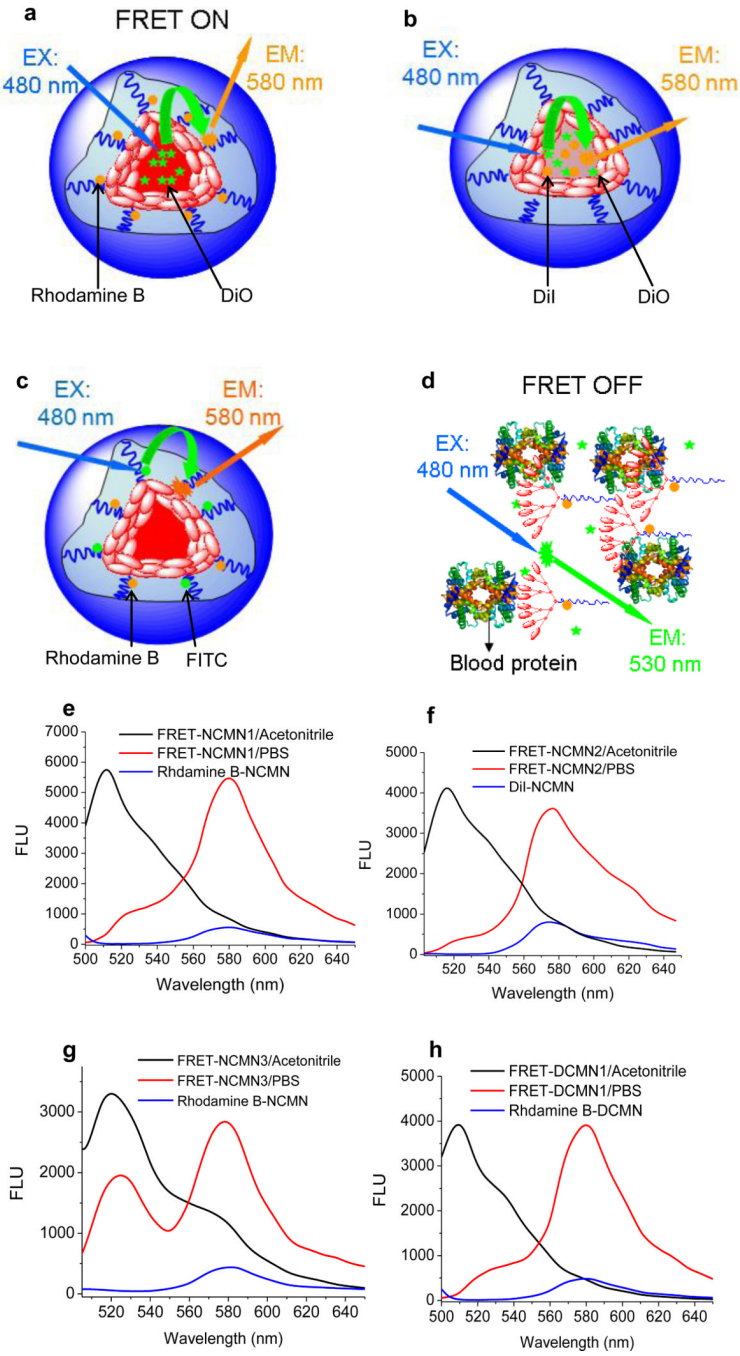

Fig. 9.

Schematic illustration of non-crosslinked FRET-based nanoparticles FRET-NCMN1 (DiO and rhodamine B pair) (**a**), FRET-NCMN2 (DiO and DiI pair) (**b**), FRET-NCMN3 (FITC and rhodamine B pair) in PBS (**c**) and FRET-NCMN1 (DiO and rhodamine B pair) in human plasma (**d**); representative fluorescence spectra of FRET-NCMN1 (DiO loading: 2.5%, rhodamine B conjugated PEG^{5k}-CA_8: 5.0 mg) in PBS (red line) and in acetonitrile (black line), NCMN with rhodamine B alone (rhodamine B conjugated PEG^{5k}-CA_8: 5.0 mg) (blue line) with 480 nm excitation (**e**); representative fluorescence spectra of FRET-NCMN2 (DiO loading: 2.5%, DiI loading: 2.5%) in PBS (red line) and in acetonitrile (black line),

NCMN with DiI alone (DiI loading: 2.5%) (blue line) with 480 nm excitation (**f**); representative fluorescence spectra of FRET-NCMN3 (FITC conjugated PEG^{5k}-CA_8: 5.0 mg, rhodamine B conjugated PEG^{5k}-CA_8: 5.0 mg) in PBS (red line) and in acetonitrile (black line), NCMN with rhodamine B alone (rhodamine B conjugated PEG^{5k}-CA_8: 5.0 mg) with 480 nm excitation (**g**); representative fluorescence spectra of FRET-DCMN1 (DiO loading: 2.5%, rhodamine B conjugated PEG^{5k}-Cys_4-CA_8: 5.0 mg) in PBS (red line) and in acetonitrile (black line), DCMN with rhodamine B alone (rhodamine B conjugated PEG^{5k}-Cys_4-CA_8: 5.0 mg) (blue line) with 480 nm excitation (**h**) [25]. Reprinted with permission from [25]. Copyright (2012) American Chemical Society.

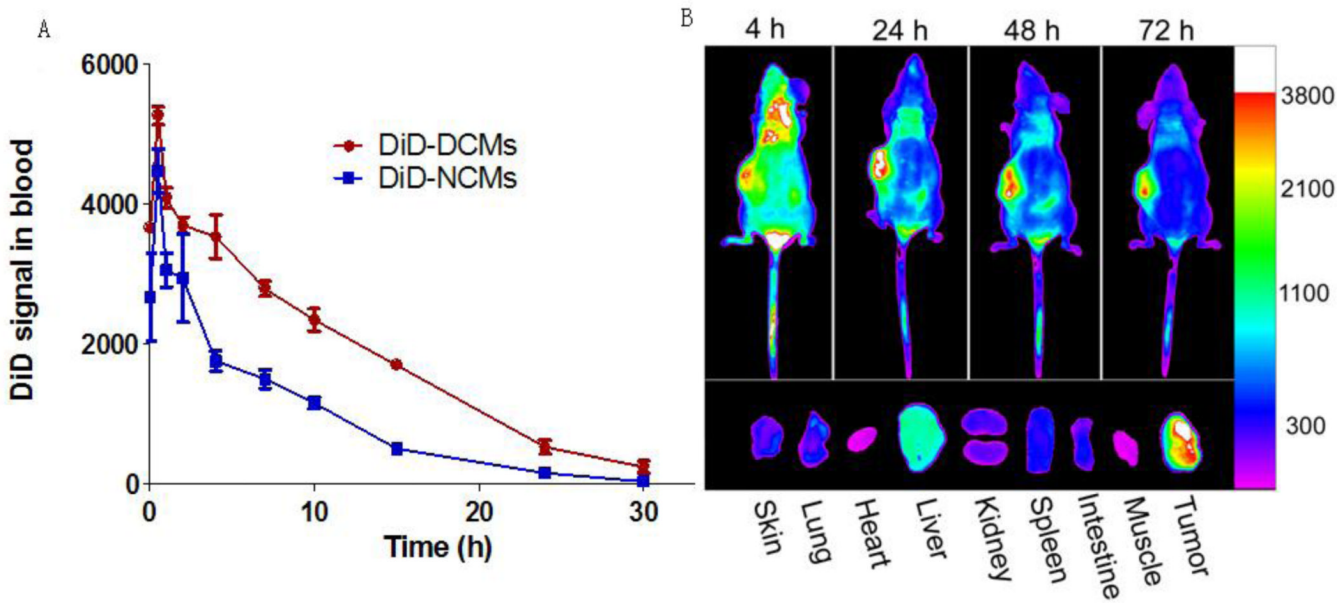

Fig. 10.

In vivo pharmacokinetics (**A**) and biodistribution (**B**) of DiD-loaded DCMs and NCMs in nude mice bearing SKOV-3 ovarian cancer xenograft [44]. Reprinted from [44], Copyright (2011), with permission from Elsevier.

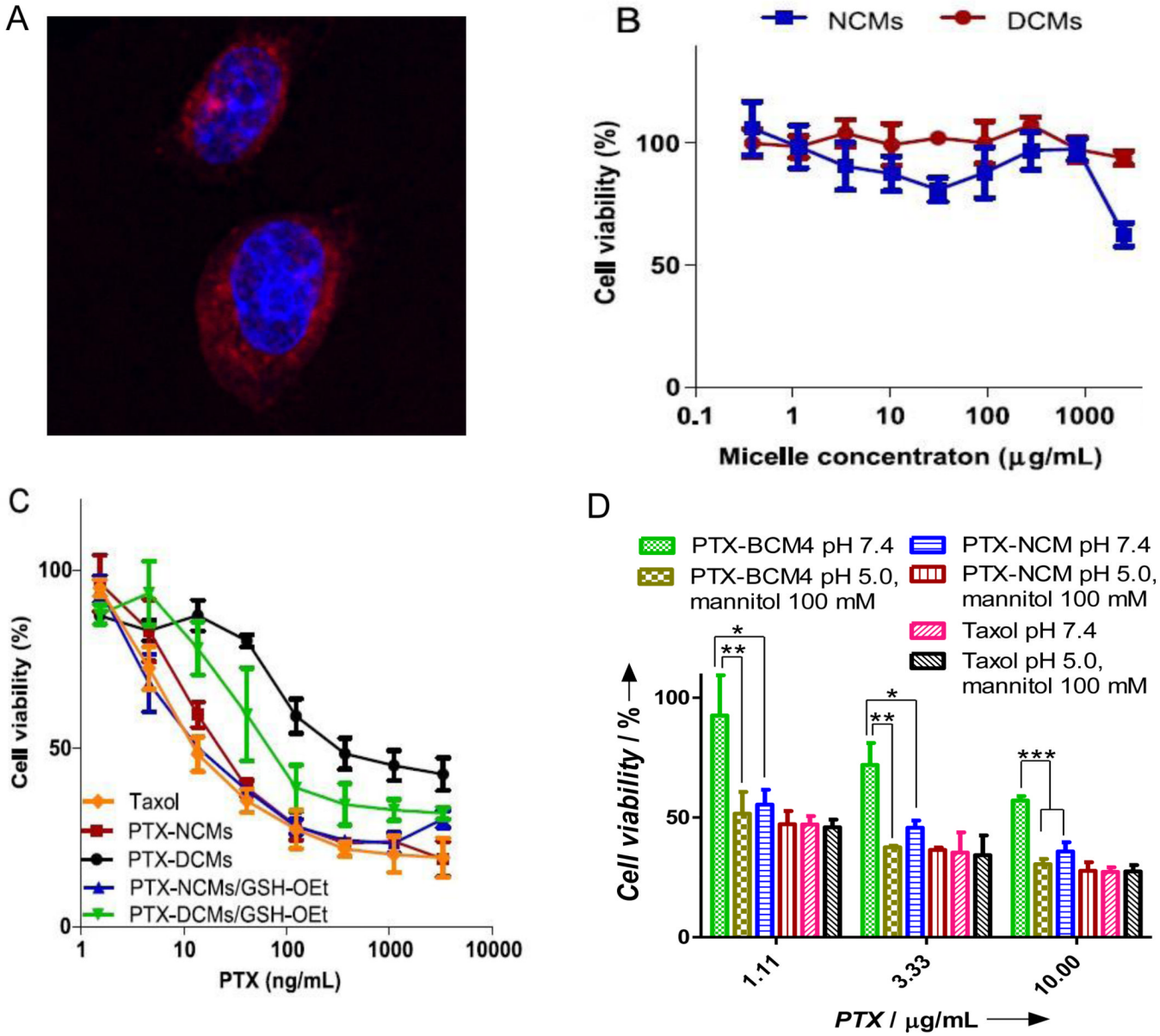

Fig. 11.

(**A**) Cellular uptake of DiD-labeled DCMs in SKOV-3 ovarian cancer cells after 3 h incubation time, observed by confocal microscopy. The cell viability of SKOV-3 cells treated with (**B**) different concentrations of blank NCMs and DCMs, (**C**) Taxol®, PTX-NCMs and PTX-DCMs with and without pretreatment of 20 mM GSH-OEt, and (**D**) Taxol®, PTX-NCMs and PTX-BCM4 with or without treatment with 100 mM mannitol at pH5.0 [43, 44]. Copyright Wiley-VCH Verlag GmbH & Co. KGaA. Reproduced with permission from [43]. Reprinted from [44], Copyright (2011), with permission from Elsevier.

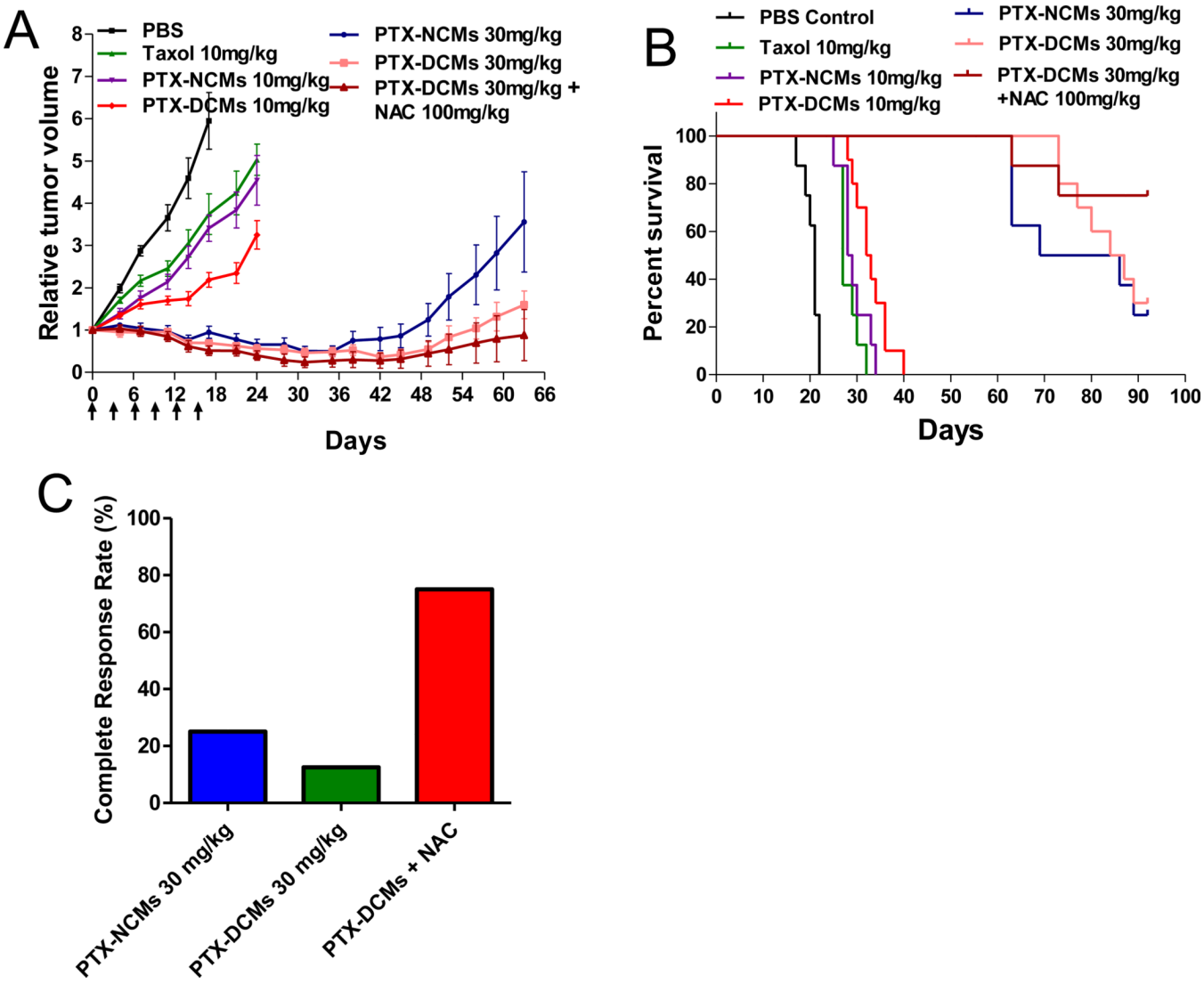

Fig. 12.

(**A**) *In vivo* anti-tumor efficacy after intravenous treatment of different PTX formulations in the subcutaneous mouse model of SKOV-3 ovarian cancer. Tumor bearing mice were administered i.v. with PBS (control) and different PTX formulations on days 0, 3, 6, 9, 12, 15 when tumor volume reached about 100~200 mm^3 (n=8). (**B**) Survival of mice in different treatment groups. (**C**) Complete tumor response rate of mice treated with 30 mg/kg PTX-NCMs and PTX-DCMs with or without the trigger release by NAC [44]. Reprinted from [44], Copyright (2011), with permission from Elsevier.

Table 1

An overview of the reported stimuli responsive crosslinked micelle systems.

Assembly Units	Crosslink Strategy	Stimuli	Payload	Particle size (nm)	Ref.
Poly(amidoamine)-cholesterol conjugates	disulfide	reduction	azobenzene, estradiol	100–300	[75]
PCL-b-PPESH-b-PEG	disulfide	reduction	doxorubicin	50	[54]
PEG-b-PLys-b-PPha	disulfide	reduction	methotrexate	25–50	[35]
PEI-(bromomethyl)phenylboronic acid	disulfide	reduction	pGL3 gene	200–300	[76]
PEG-oligocholic acids (CA)	disulfide	reduction	paclitaxel	28	[44]
PEG-oligocholic acids (CA)	disulfide	reduction	vincristine	16	[55]
PEI	disulfide	reduction	DNA		[56]
PEG-P(Lys)/ PEG-P(Asp)	disulfide	reduction	siRNA	16	[77]
PEG-PLL	disulfide	reduction	pDNA	100	[78]
PEG-*b*-(PLL-IM)	disulfide	reduction	siRNA	60	[58]
PEG-L_2-PCL	disulfide	reduction	doxorubicin	20–150	[79]
Dextran-lipoic acid derivatives	disulfide	reduction	doxorubicin	20–35	[29]
mPEG-Cys-PCL	disulfide	reduction	doxorubicin	191	[47]
Thiolated c(RGDfK)-poly(ethylene glycol)-*b*-poly(lysine) (PEG-PLys),	disulfide	reduction	pDNA	110	[80]
poly(L-cysteine)-*b*-poly(L-lactide)/ PLC-*b*-PLLA	disulfide	reduction		50	[81]
PEG-*b*-P(DEA-*s*-TMSPMA)	siloxane	pH		250	[82]
PEO-*b*-P(NIPAM-*co*-NAS)	Cystamine	temperature and reduction		50–120	[41]
P(NIPAAm-co-MPMA)-b-P(DEA)	silica-based cross-linking	temperature and pH	prednisone	70–220	[83]
$PAGA_{180}$-b-$PNIPAAM_{350}$	covalent	temperature and pH		85–310	[67]
poly(hydroxyethyl acrylate)-poly(butyl acrylate) (PHEA)-*b*-PBA)	divinyl acid labile crosslinker	pH	doxorubicin	40–260	[40]
PEG-oligocholic acids (CA)	boronate	pH, cis-diol	paclitaxel	22–27	[43]
PEO-b-PMA/Ca_{2+}	disulfide	reduction	doxorubicin	100–300	[59]
mPEO-PAPMA-PDPAEMA	disulfide	pH, reduction		120–220	[63]
mPEG-Asp(MEA)-PAsp(DIP)	disulfide	pH, reduction	doxorubicin	45–550	[62]

Assembly Units	Crosslink Strategy	Stimuli	Payload	Particle size (nm)	Ref.
mPEG-b-p(HEMA$_m$-Lac$_n$)	hydrazone linker	hydrolysable	doxorubicin	68	[26, 46, 49]
PEG-PAsp-PPhe	ketal-containing cross-linkers	hydrolysable	doxorubicin	50–55	[50]
P(AMPS-b-AAL))	interpolyelectrolyte	pH/Salt		27–70	[60]
PDMAEMA$_{54}$-*b*-P(MMA$_{55}$-*co*-MMA$_{19}$)	photoinduced dimerization of coumarin groups	temperature and pH		30–50	[66]
mPEO-PAPMA-PDPAEMA	imine	temperature and pH	prednisolone 21-acetate	80–95	[61]